Am J Transl Res 2022;14(8):5308-5325
www.ajtr.org /ISSN:1943-8141/AJTR0143170

Original Article

A novel immune prognostic model of non-M3 acute myeloid leukemia

Hong Ding[1], Yu Feng[1], Juan Xu[1], Zhimei Lin[1,2], Jingcao Huang[1], Fangfang Wang[1], Hongmei Luo[1], Yuhan Gao[1], Xinyu Zhai[1], Xin Wang[1], Li Zhang[1], Ting Niu[1], Yuhuan Zheng[1]

[1]*Department of Hematology, West China Hospital, Sichuan University, Chengdu 610041, Sichuan, China;*
[2]*Department of Hematology, The Affiliated Hospital of Chengdu University, Chengdu 610081, Sichuan, China*

Received March 28, 2022; Accepted July 3, 2022; Epub August 15, 2022; Published August 30, 2022

Abstract: Acute myeloid leukemia (AML) is a common hematological malignancy in adults. AML patients exhibit clinical heterogeneity with complications of molecular basis. The leukemogenesis of AML involves immune escape, and the immunosuppression status of the patient might have great impact on AML treatment outcome. In this study, we established an immune prognostic model of AML using bioinformatics tools. With the data in the TCGA and GTEx datasets, we analyzed differentially expressed genes (DEGs) in non-M3 AML and identified 420 immune-related DEGs. Among which, 49 genes' expression was found to be related to AML prognosis based on univariate Cox regression analysis. Next, we established a prognostic model with these 49 genes in AML by LASSO regression and multivariate Cox regression analyses. In our model, the expressions of 5 immune genes, MIF, DEF6, OSM, MPO, AVPR1B, were used to stratify non-M3 AML patients' treatment outcome. A patient's risk score could be calculated as Risk Score=0.40081 × MIF (MIF expression) - 0.15201 × MPO + 0.78073 × DEF6 - 0.45192 × AVPR1B + 0.25912 × OSM. The area under the curve of the risk score signature was 0.8, 0.8, and 0.96 at 1 year, 3 years, and 5 years, respectively. The prognostic model was then validated internally by TCGA data and externally by GEO data. At last, the result of single-sample gene-set enrichment analysis demonstrated that compared with healthy samples, the abundance of non-turmeric immune cells was significantly repressed in AML. To summarize, we presented an immune-related 5-gene signature prognostic model in AML.

Keywords: Acute myeloid leukemia, bioinformatics, nomogram, prognosis

Introduction

Acute myeloid leukemia (AML) is a common myeloid carcinoma with high heterogeneity [1, 2]. Based on the French-American-British (FAB) classification system, AML is generally classified into 8 subtypes according to the leukemia cells' morphology and cytogenetic characteristics of leukemic cells in hemogram and myelogram [2]. Different subtypes of AML have different prognosis. After the use of all-trans retinoic acid clinically, acute promyelocytic leukemia (APL) becomes the most curable subtype of AML with a cure rate of 80% [3, 4]. However, for patients with other subtypes of AML, the 5-year overall survival (OS) is approximately 45% in young patients (≤ 60 years old), whereas it is less than 10% in old patients (> 60 years old) [5]. Thus, AML patients' stratification and accurate treatment regimen selection remain important topics for researchers and clinical specialists.

It has long been recognized that immune features of AML patients affect the prognosis [6, 7]. A previous study demonstrated that adult AML patients with high level of IgA2 B cells were related to poor OS [7]. In addition, $TIGIT^+$ natural killer (NK) cells were related to poor outcome in AML patients [8]. On the other hand, immunotherapy, such as CD33 monoclonal antibody, has been used in AML treatment and showed promising in some patients. Other immunotherapies, including chimeric antigen receptor (CAR) T cell and bispecific T cell engagers (BiTEs), are widely tested in different clinical trials. European Leukemia Net (ELN) recommendations, which are based on cytogenetic abnormalities and genetic mutations, are com-

monly used hazard stratification in AML. To our knowledge, there is no recommended AML prognostic model that was based on immune genes expression. In this study, we established an immune model to predict AML treatment outcome. The model itself, as well as identified key genes expression, might help to improve AML immunotherapy.

Materials and methods

Data acquirement

RNA sequencing data of AML were acquired from the TCGA database (https://portal.gdc.cancer.gov/repository) and the GEO database (https://www.ncbi.nlm.nih.gov/geo/). The GTEx database (https://www.gtexportal.org/home/) was conducted to download gene expression data for 337 normal whole blood cell samples. The training data of 116 non-M3 AML patient samples were collected from TCGA-LAML, after excluding patient with incomplete clinical information. An external verification was performed using GSE37642 data from GEO. The immune-related genes (IRGs) were obtained from the ImmPort database (https://www.immport.org/).

Screening differentially expressed genes

Data processing and analysis were based on R (Version 4.1.0). The count matrices of the TCGA and GTEx datasets were converted to raw counts, and then the "cpm" function of "edgeR" package removed the bias of the library sequencing depth. After intersection, 26792 genes were obtained between AML patient samples and normal whole blood control samples. Gene difference analysis was conducted with the "limma", "DSeq2" and "edgeR" packages, and genes with a Log_2 |Fold Change| of > 2 and P value ≤ 0.05 were identified as the differentially expressed genes (DEGs). Visualize DEGs obtained in 3 packages with "VennDiagram" package, and we used the "union" function to merge the genes. Immune-related DEGs in AML were obtained by intersecting DEGs with IRGs

Biological functions and enrichment analysis

Enrichment analyses, including Gene Ontology (GO) functional enrichment analysis, Kyoto Encyclopedia of Genes and Genomes (KEGG) analysis and Gene Set Enrichment Analysis (GSEA), of DEGs and AML-immune-related DEGs were conducted with the "cluster Profiler" [9], "enrichplot" and "org.db.hus" packages of R. "Immunologic signature gene sets" and "hallmark gene sets" (http://www.gsea-msigdb.org/gsea) from GSEA were used.

Establishment and validating an immune prognostic model in AML

The correlation between target gene expression and OS of AML patients was analyzed using univariate Cox regression with R packages "survival", "glmnet", "survminer", "My.stepwise". Then we used LASSO regression analysis to identify candidate genes for the risk score signature. At last, a multivariate Cox regression analysis was performed to investigate candidate genes and establish the prediction model.

To validate the prognostic model with training dataset from TCGA as described earlier, non-M3 AML patients (n=116) were randomly separated into two parts according to a proportion of 1:1, and one group was defined as an internal validation dataset. For external validation, GSE37642 dataset from GEO was used. R packages used in survival analysis were "survival", "glmnet", "survminer", "My.stepwise", etc.

Mutation profiles analysis

Somatic mutation profiles of 51 none-M3 AML patients were obtained from TCGA. In addition, the waterfall plot showing the mutations were generated and analyzed by "maftools" R package.

Evaluation of tumor microenvironment immune cell infiltration

The abundance of non-turmeric cells in PBMCs of AML patients was analyzed as previous described [10]. A genomic set of immune cells was established according to Pornpimol Charoentong [11]. The single-sample gene-set enrichment analysis (ssGSEA) algorithm [12], which standardized the rank of genes expression in a specified sample and calculated the enrichment score with the use of the empirical cumulative distribution function, was used to evaluate the difference of enriched immune

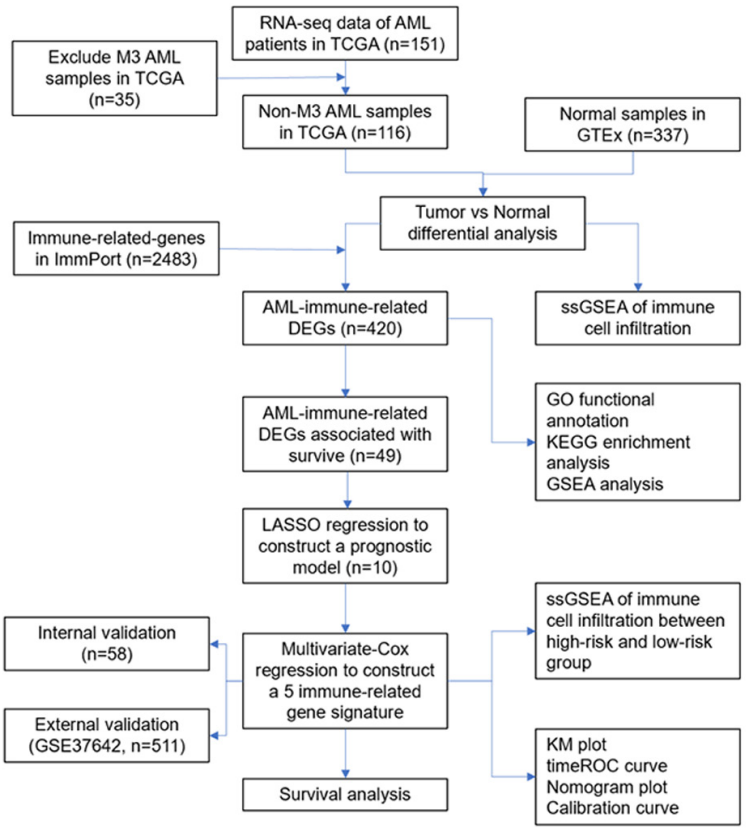

Figure 1. The flow chart of establishing and validating an immune prognostic model in AML.

Table 1. Clinical characteristics of non-M3 AML patients in the TCGA-LAML dataset

	Number	Percentage (%)
FAB category		
M0	12	10.3%
M1	31	26.7%
M2	31	26.7%
M4	27	23.3%
M5	12	10.3%
M6	2	1.7%
M7	1	0.9%
Gender		
male	64	55.2%
female	52	44.8%
Survival status		
dead	75	64.7%
alive	41	35.3%
Age (years)		
> 57	55	47.4%
≤ 57	61	52.6%
Median (range)	57 (21-88)	
Overall survival days (median)	365	

cells in tumor microenvironment (TME) between normal and AML samples. The ssGSEA was also applied for non-M3 AML patients' data to perform immunocytroverance assessment to compare Cox prognostic risk score in high-risk and low-risk groups [13, 14]. The principal component analysis (PCA) was used to reduce the dimension of the data, mainly through linear transformation to transform the original data into a group of linearly independent data, followed by extraction of the main feature components, so as to roughly judging the quality of the data. "GSVA", "estimate" and "pheatmap" R packages were used.

Statistical analysis

All statistical analyses were conducted with R software (version 4.1.0). Based on the median hazard score, the patients were separated into high-risk group and low-risk group. DEGs were identified using students' t-test. The Kaplan-Meier (KM) curve was conducted to show the prognosis of two groups of patients. Analyzing KM survival curves required the log-rank test. And the area under the curve (AUC) of the receiver operating characteristic (ROC) curve was conducted to assess the quality of the model by "timeROC" packages. We calculated correlations with Spearman's correlation coefficients. A P value < 0.05 is considered statistically significant in all analyses.

Results

Identification of differentially expressed immune-related genes in AML

The research flow chart was shown in **Figure 1**. The DEGs between non-M3 AML patients and healthy individuals were screened as described in Method and Materials section. A summary of the basal clinical information of non-M3 patients from the TCGA-LAML dataset was presented in **Table 1**. The quality of original RNA sequencing data used in our study was ana-

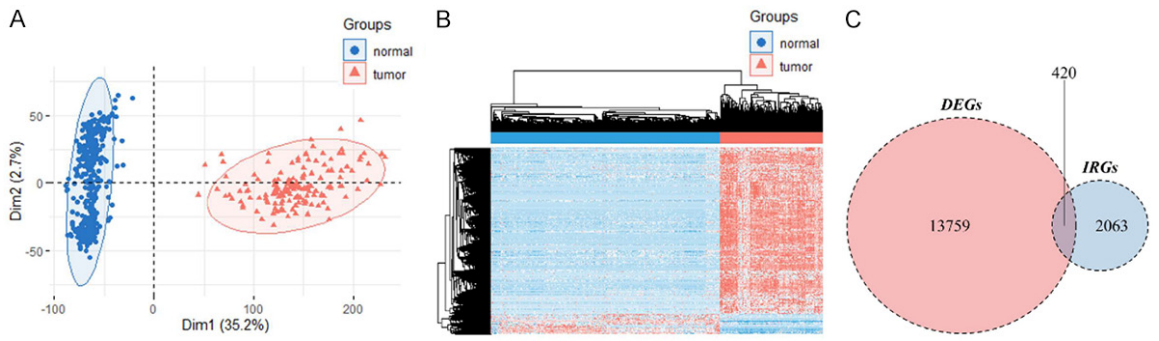

Figure 2. Identification of differentially expressed immune-related genes in AML. A. Principal component analysis plot of normal and AML samples; B. Heatmap of differentially expression genes (DEGs) between normal and AML samples; C. Venn diagrams of immune-related genes (IRGs) and DEGs.

lyzed by PCA (**Figure 2A**). AML and healthy individuals exhibited significantly different patterns of gene expression. As exemplified in a heatmap in **Figure 2B**, there were 14179 DEGs identified in AML, of which 11877 were upregulated and 2302 were downregulated. Next, we further extracted IRGs in DEGs. The list of IRGs, which comprised a total of 2483 IRGs and covered 17 immune categories, was obtained from ImmPort as described earlier [15]. After intersection of DEGs and IRGs, we found 420 differentially expressed IRGs in AML (**Figure 2C**). Detailed information of AML immune-related DEGs was presented in Table S1.

Next, we conducted GO and KEGG enrichment analyses with those 420 immune-related DEGs. In GO enrichment, the enriched pathways were categorized into molecular functions (MFs), cellular components (CCs) and biological processes (BPs). The top three enriched pathways in BPs were humoral immune response, cell chemotaxis and leukocyte chemotaxis. The top three enriched pathways in CCs were T-cell receptor complex, plasma membrane signaling receptor complex and immunoglobulin complex. And the top three enriched pathways in MFs were signaling receptor activator activity, receptor ligand activity, and cytokine activity (**Figure 3A**, **3B**). In addition to annotating the function of genes, KEGG enrichment also showed relationship between genes and signaling pathways. The KEGG analysis results of immune-related DEGs revealed a high correlation with cytokine-cytokine receptor interaction, viral protein interaction with cytokine and cytokine receptor, chemokine signaling pathway (**Figure 3C**, **3D**). In addition, GSEA enrichment provided alternative gene and pathway classification. Therefore, we performed GSEA pathway enrichment with 420 immune-related genes. Those 420 differentially expressed IRGs in AML were enriched in KRAS signaling, L6-JAK-STAT signaling and allograft rejection pathways in GSEA HALLMARK gene sets (**Figure 3E**). Specifically, we used immunologic signature gene sets in GSEA to analyze immunological pathway enrichment. A total of 36 immunological pathways were significantly enriched, with top 3 enrichments were NAÏVE BCELL vs NEUTROPHIL, HEALTHY vs RSV INF PBMC, CYANOBACTERIUM LPSLIKE vs LPS AND CYANOBACTERIUM LPSLIKE STIM DC 3H pathways (**Figure 3F**). More information of GSEA pathway enrichment was presented in Table S2. To summarize, with published gene expression data, we identified DEGs in AML. We selected immune-related genes in DEGs and analyzed those genes' enrichment in pathways.

The results of differential gene enrichment analysis revealed diverse signaling pathways related to cytokines. Of notice, many identified differentially regulated IRGs, such as IL-10, TGF-β, and IFN-gamma, had been shown to function as immunosuppressive factors in AML or other human cancers. Tumor cells could secrete chemokines to stimulate immune cell migration, thus modulated the infiltration of immune cells in TME. AML could recruit immunosuppressive cells, such as myeloid-derived suppressive cells (MDSCs), regulatory T cells (Tregs) and tumor-associated macrophages (TAMs), all of which were able to release cytokines that suppress the immune system [16-

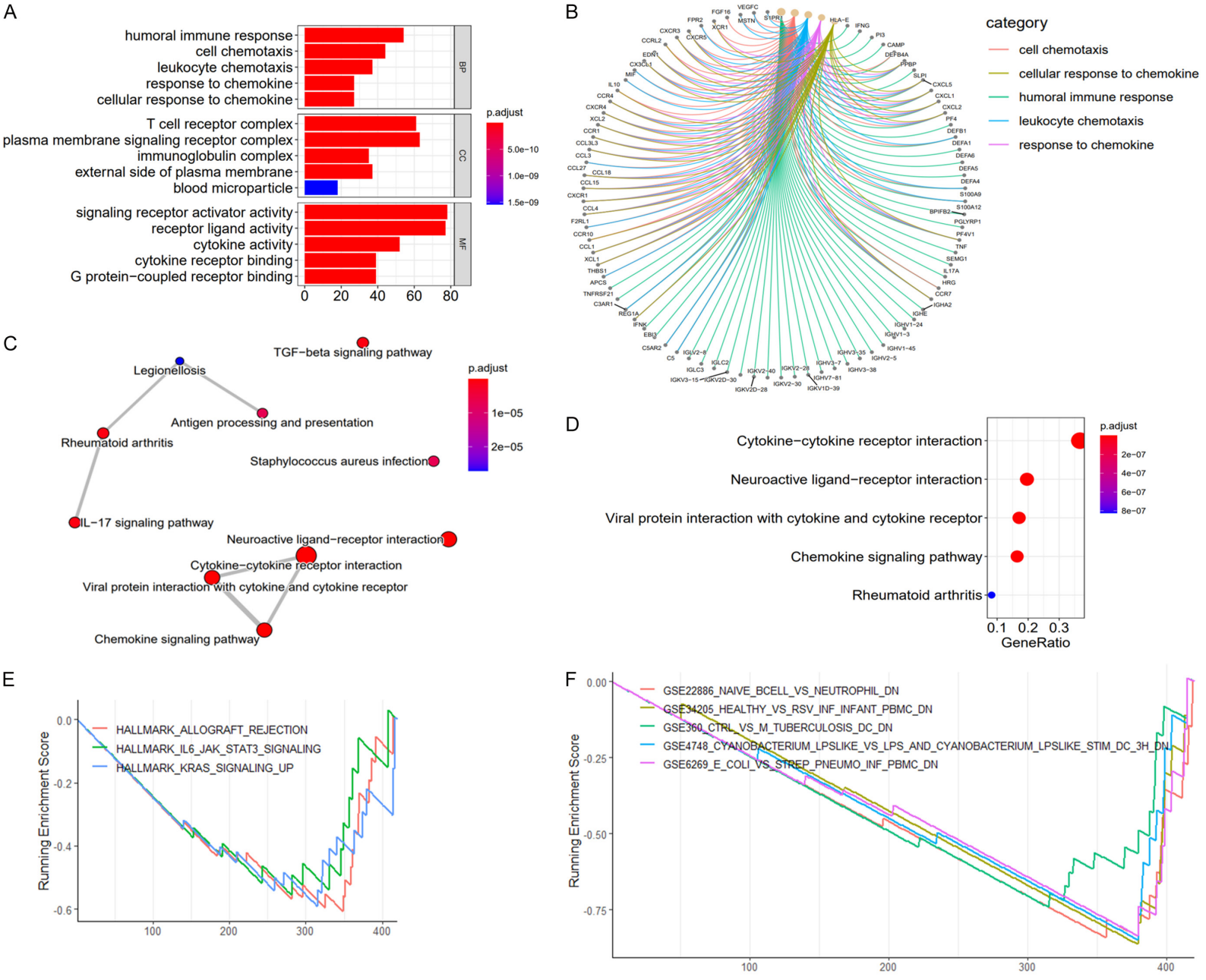
A
humoral immune response
cell chemotaxis
leukocyte chemotaxis
response to chemokine
cellular response to chemokine
T cell receptor complex
plasma membrane signaling receptor complex
immunoglobulin complex
external side of plasma membrane
blood microparticle
signaling receptor activator activity
receptor ligand activity
cytokine activity
cytokine receptor binding
G protein−coupled receptor binding
BP
CC
MF
p.adjust
5.0e−10
1.0e−09
1.5e−09
0
20
40
60
80
B
category
cell chemotaxis
cellular response to chemokine
humoral immune response
leukocyte chemotaxis
response to chemokine
C
TGF−beta signaling pathway
Legionellosis
Antigen processing and presentation
Rheumatoid arthritis
Staphylococcus aureus infection
IL−17 signaling pathway
Neuroactive ligand−receptor interaction
Cytokine−cytokine receptor interaction
Viral protein interaction with cytokine and cytokine receptor
Chemokine signaling pathway
p.adjust
1e−05
2e−05
D
Cytokine−cytokine receptor interaction
Neuroactive ligand−receptor interaction
Viral protein interaction with cytokine and cytokine receptor
Chemokine signaling pathway
Rheumatoid arthritis
p.adjust
2e−07
4e−07
6e−07
8e−07
0.1
0.2
0.3
GeneRatio
E
HALLMARK_ALLOGRAFT_REJECTION
HALLMARK_IL6_JAK_STAT3_SIGNALING
HALLMARK_KRAS_SIGNALING_UP
Running Enrichment Score
0.0
-0.2
-0.4
-0.6
100
200
300
400
F
GSE22886_NAIVE_BCELL_VS_NEUTROPHIL_DN
GSE34205_HEALTHY_VS_RSV_INF_INFANT_PBMC_DN
GSE360_CTRL_VS_M_TUBERCULOSIS_DC_DN
GSE4748_CYANOBACTERIUM_LPSLIKE_VS_LPS_AND_CYANOBACTERIUM_LPSLIKE_STIM_DC_3H_DN
GSE6269_E_COLI_VS_STREP_PNEUMO_INF_PBMC_DN
Running Enrichment Score
0.00
-0.25
-0.50
-0.75
100
200
300
400

Figure 3. Enrichment analysis of AML-immune-related DEGs. A. Barplot of Gene Ontology (GO) biological functions analysis; B. Circular cnetplot of GO pathways; C. Emapplot of Kyoto Encyclopedia of Genes and Genomes (KEGG) pathways; D. Dotpplot of KEGG enrichment analysis; E. Enrichment plot of Hallmark pathways; F. Enrichment plot of Immunologic pathways.

20]. There were evidences that TGF-β and IL-10 could suppress T cell activation and proliferation [21, 22]. In addition, by binding to membrane-bound TGF-β, Tregs suppressed the functions of dendritic cells and the cytotoxicity of NK cells [23-26]. When stimulated by Galectin-9, NK cells produced IFN-gamma, which was an enzyme responsible for the breakdown of tryptophan, then tryptophan consumption and its metabolites would lead to T-cell apoptosis [27, 28]. PD-L1 could also be induced by IFN-gamma, allowing AML cells to escape immune surveillance [29-32].

Establishing and validating an immune prognostic model in AML

We started with 420 immune-related DEGs in AML and examined the correlation between each gene's expression and AML OS. The result of univariate Cox regression analysis suggested that 49 gene's expression each correlated with AML OS ($P < 0.05$, Figure S1A). Next, we generated a prognostic model using LASSO regression analysis with of these 49 prognostic genes. A total of 10 genes were identified as potential candidate genes according to the optimal value of λ (**Figure 4A**, **4B**). The AUC of LASSO regression prognostic model was 0.757 (Figure S1B). Next, we conducted multivariate Cox regression analysis of those 10 genes, and identified a 5-gene signature in AML prognosis prediction with a C-index of 0.72 (**Figure 4C**). Those genes were *MIF*, *MPO*, *DEF6*, *AVPR1B*, and *OSM*. In order to calculate risk scores, the following formula was used: Risk Score= 0.40081 × MIF (MIF expression) - 0.15201 × MPO + 0.78073 × DEF6 - 0.45192 × AVPR1B + 0.25912 × OSM. Time-ROC curve demonstrated that the AUC of the model was 0.8, 0.8, and 0.96 at 1 year, 3 years, 5 years, respectively (**Figure 4D**).

To examine the risk-stratification efficiency of our model, we calculated risk scores for each of 116 AML patients from TCGA, and divided the patients into high-risk and low-risk groups with the median value. According to the KM curve, high-risk patients had a significantly shorter OS than low-risk patients ($P < 0.0001$, **Figure 4E**). As exemplified in **Figure 4F**, **4G**, MIF, DEF6, OSM were upregulated in high-risk group, while MPO and AVPR1B were downregulated. In addition, the result of nomogram also indicated that the 5-gene signature could predict the survival of non-M3 AML patients with a C-index of 0.72 (**Figure 5A**, **5B**). The prognostic model showed effective in different stage, gender, age, cytogenetic background groups of patients (**Figure 5C**). More information about above univariate Cox regression analysis was presented in Table S3.

Next, we evaluated our prognostic model with an internal validation and an external validation. For internal validation, we randomly divided non-M3 AML patients (n=116) from TCGA into two groups, the training set and test set, with the proportion of 1:1. The AUC of risk scores at 1 year, 3 years, and 5 years were 0.81, 0.78, and 0.92, respectively (**Figure 6A**). For external validation, we used GSE37642 dataset. The clinical information of patients in GSE37642 was presented in **Table 2**. KM curve demonstrated that high-risk patients had a noticeably shorter OS than low-risk patients (**Figure 6B**). And the AUCs were 0.66, 0.7, and 0.74 at 1 year, 3 years, and 5 years, respectively (**Figure 6C**). Overall, our 5-gene model provided good performance in AML prognosis prediction.

Mutation profiles in non-M3 AML

We also examined mutation profiles of non-M3 AML with published dataset in TCGA. As exemplified in **Figure 7A**, missense mutations were the most common genetic aberration in AML. Single nucleotide polymorphism was also common in non-M3 AML, with C > T was identified as the most prevalent single nucleotide variants (**Figure 7B**, **7C**). The number of mutations in each patient was summarized in boxplot in **Figure 7D**. Top 10 mutated genes in non-M3 AML were exhibited in **Figure 7E**. Those genes were *DNMT3A*, *RUNX1*, *NPM1*, *FLT3*, *IDH2, KIT, TP53, TTN, MUC16,* and *NRAS.*

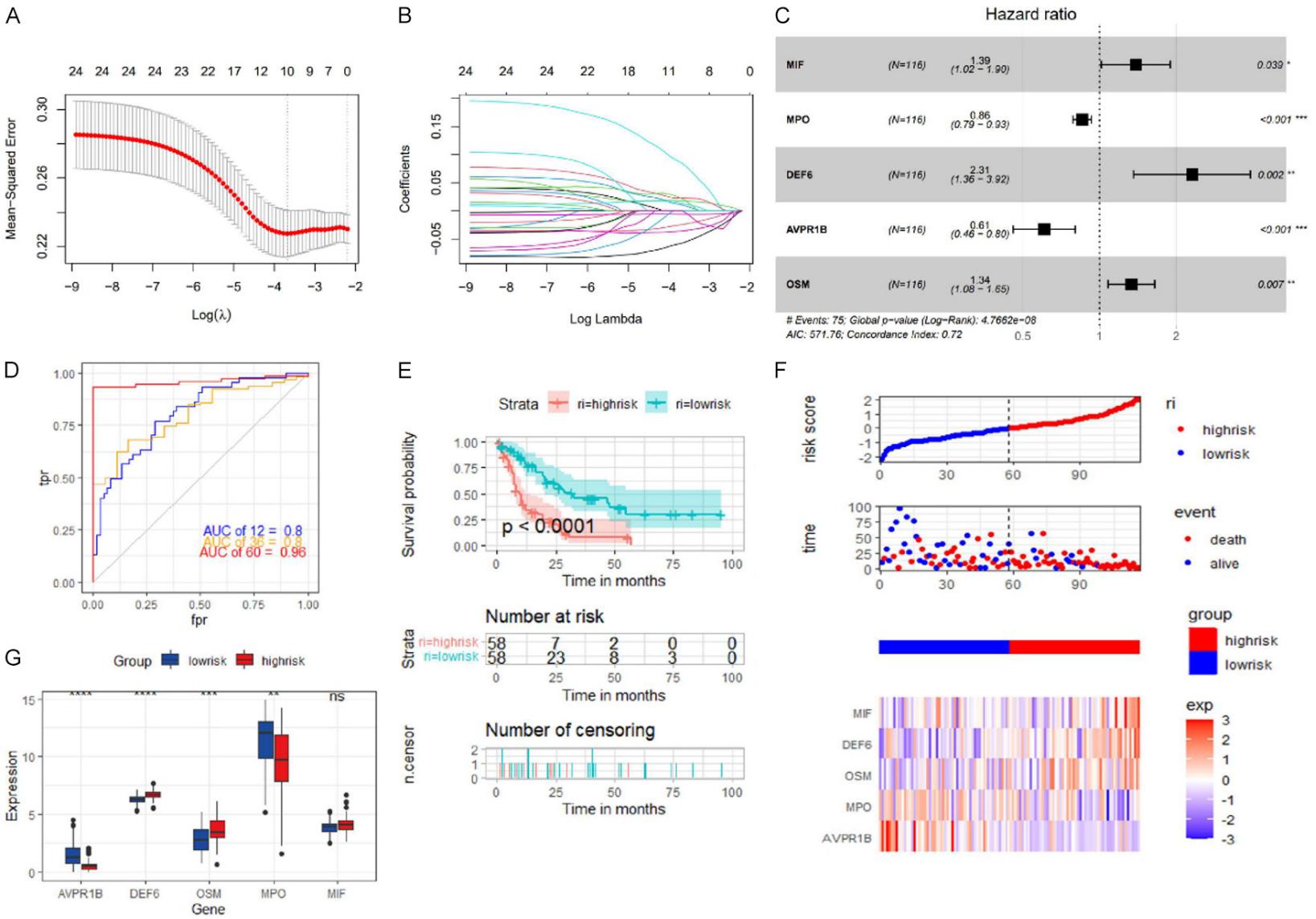

Figure 4. Establishing an immune-related prognostic model in AML. A, B. Lasso regression of 49 AML-immune-related DEGs; C. Forest plot of multivariate Cox regression analysis; D. Time ROC curve of multivariate Cox regression; E. Kaplan-Meier (KM) curve between the high-risk group and low-risk group; F. The relationship between the risk score, overall survival, living status and the expression of 5 immune signatures; G. The expression level of 5 IRGs between the high-risk and low-risk group (**P < 0.01, ***P < 0.001, ****P < 0.0001).

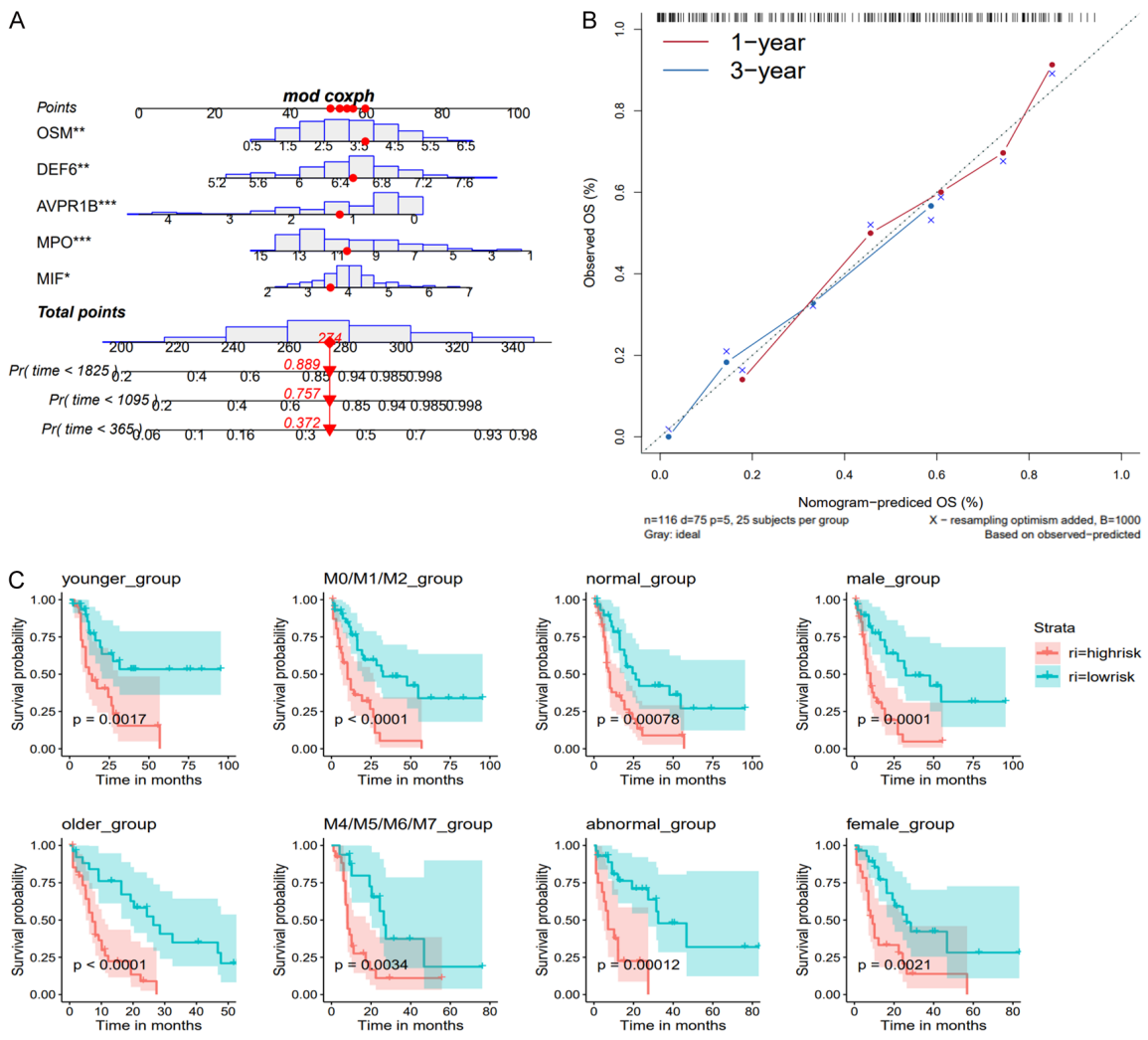

Figure 5. Results of multivariate Cox regression analysis. A. Nomogram plot; B. The calibration curve of nomogram plot; C. Survival analysis of 8 clinical subgroups according to risk scores.

Evaluation of immune cell infiltration in AML tumor microenvironment

According to ssGSEA analysis, most non-malignant cells were differentially infiltrated in AML samples versus healthy samples, except for immature B cell (**Figure 8A**). We investigated the immune activity and stromal activity in AML TME by the ESTIMATE algorithm [45]. The result demonstrated that immune and stromal activities were noticeably repressed in AML (**Figure 8B**). We also conducted correlation analyses to determine whether there was a relationship between risk scores and the type of TME cells in APL patients. As exemplified in **Figure 8C**, a positive correlation between risk scores and TME cell infiltration was observed in central memory CD8 T cell, T follicular helper cell, active CD4 T cell, active B cell, type 1 T helper cell, MDSC, neutrophil, immature B cell, Tregs, monocyte, NK T cell, CD56 bright NK cell, effector memory CD4 T cell and macrophage. For the purpose of exploring the relationship between target genes and TME infiltrating cells, we conducted spearman correlation analyses and found that DEF6 was positively correlated with the majority of the TME infiltrating immune cells, while AVPR1B was negatively correlated (**Figure 8C**). In summary, non-tumor immune cells were remarkably reduced in AML samples compared to healthy controls. This finding deserves further investigation.

Discussion

Immunotherapy has achieved good results in many human cancers [46-48]. In AML, alloge-

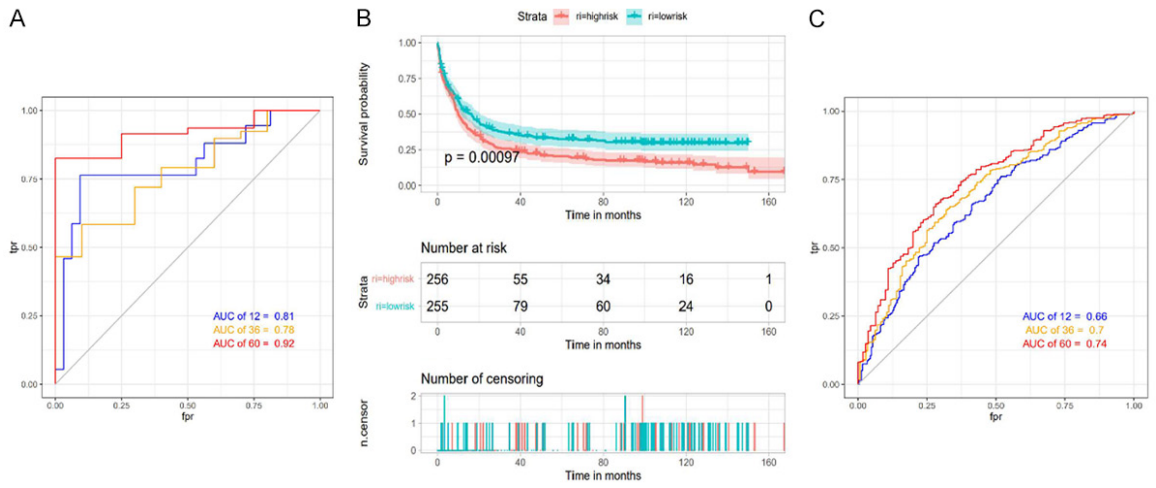

Figure 6. Validation of the immune-related AML prognostic model. A. Time ROC curve of the internal validation; B. KM curve of GSE37642; C. Time ROC curve of external validation.

Table 2. Clinical characteristics of non-M3 AML patients in the GSE37642 dataset

	Number	Percentage (%)
FAB category		
M0	22	4.3%
M1	113	22.1%
M2	164	32.1%
M4	121	23.7%
M5	66	12.9%
M6	22	4.3%
M7	3	0.6%
Survival status		
dead	382	74.8%
alive	129	25.2%
Age (years)		
> 57	251	49.1%
≤ 57	260	50.9%
Median (range)	58 (18-85)	
Overall survival days (median)	342	

neic hematopoietic stem cell transplantation (alloHSCT) is the earliest and the most effective immunotherapy [49]. Emerging immunotherapy, such as CD33 monoclonal antibody has been shown to reduce recurrence risks of AML and improve outcomes among some patients [50, 51]. At present, anti-CD33 monoclonal antibody is mainly used in newly diagnosed $CD33^+$ AML patients, including those with favorable or intermediate cytogenetic risk profiles, or elderly patients (> 60 years) without actionable mutations who are not suitable for induced remission therapy. CD33 monoclonal antibody can also be used to treat CD33 positive relapsed/refractory AML patients [52, 53]. In addition, many AML immunotherapy agents including immune checkpoint inhibitors [54], target antigen antibodies [55], and CAR-T cells have been developed and validated in pre-clinical and clinical stages [56]. However, because of the low mutation load, strong immunosuppression and low immunogenicity of tumor cells in AML patients, scientists have difficulties to identify antigen-specific cytotoxic immune cells for AML treatment [57]. In addition, the heterogeneity nature of AML also caused different responses to immunotherapy in patients. At present, the optimal single therapeutic target of AML has yet been identified. Most AML immunotherapies are used in conjunction with conventional therapies including chemotherapy and HSCT [53].

According to patients' cytogenetic and molecular characteristics, ELN stratifies AML patients into three risk layers: poor, intermediate and favorable. Such stratification is also used to guide treatment and to predict prognosis [58]. Modifications of ELN stratification with additional clinical information, such as age and minimal residual disease status, result in better prediction of AML outcome [59, 60]. Of notice, immune microenvironment is important for the development and treatment of AML [57], in particular in the era of AML immu-

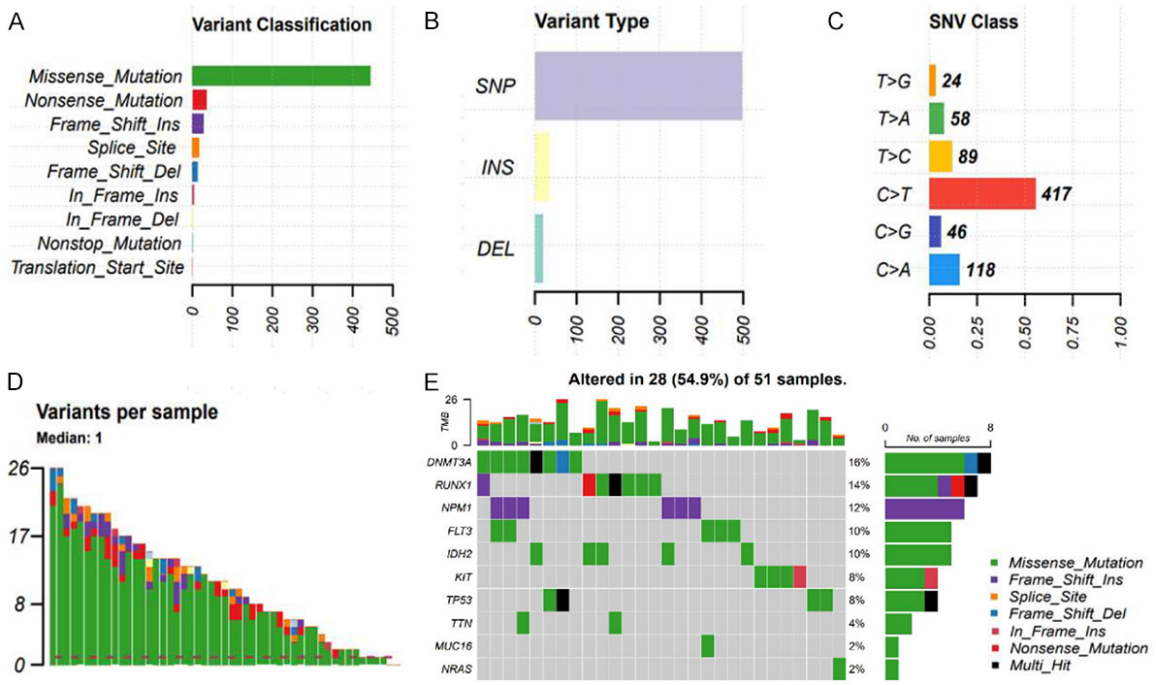

Figure 7. Mutation profiles in non-M3 AML patients. A-C. Various classifications of mutation based on different groups; D. Burden of tumor mutation in selected samples; E. Waterfall plot of the mutation details.

notherapy. It might be interesting to develop immune-related prognostic model in AML and evaluate its significance. In this study, we first screened AML-specific IRGs, and then identified OS correlated IRGs. At last, we conducted LASSO regression and univariate Cox regression to generate a 5-gene panel to predict non-M3 AML prognosis. The AUC of our model was 0.8, 0.8, and 0.96 at 1 year, 3 years, 5 years, respectively in training cohort, with a C-index of 0.72. In the past decade, many models have been proposed to predict AML prognosis [10, 61, 62]. Recently, Zhu et al. identified six genes associated with immune response to predict AML prognosis, and the AUC was 0.6643 [63]. In 2021, Li et al. proposed an immune-17 signature prognostic model in AML with an AUC of 0.823 [64].

The 5-gene model, as well as related pathway enrichment, also provided molecular basis of prognosis-related immune aberrations in AML. Within the 5-gene panel, MIF and MPO have been investigated in AML. MIF is a pro-inflammatory cytokine. MIF binds to CXC-family chemokine receptors 2 and 4, and initiates cell signaling transduction in target cells [65, 66]. A previous study showed that overexpression of MIF was associated with inferior AML prognosis [67]. Mechanistically, AML-derived MIF enhanced IL-8 expression, and promoted AML tumor cell proliferation and survival [68, 69]. MPO (myeloperoxidase) is a pivotal lineage marker used for AML diagnosis [70]. A previous study showed that MPO enhanced ROS production in AML cells, and affected AML chemosensitivity [71]. High MPO expression was associated with favorable prognosis of AML [72, 73]. Within the 5-gene model, the function of AVPR1B, DEF6 and OSM in AML has yet been recognized. DEF6 is a guanine nucleotide exchange factor for RAC1 and CDC42 [74, 75]. The high level of DEF6, which contributes to the regulation of cell cycle [76], is associated with the unfavorable prognosis of various cancers, including osteosarcoma [77], clear cell renal cell carcinoma [78], ovarian carcinoma [76]. OSM is an active IL-6 family cytokine which inhibits tumor cell proliferation through the JAK/STAT3 pathway [79-81]. In addition, OSM presents essential to immune homeostasis and haematopoiesis, inflammation, so that the change of OSM activity promotes cancer [82]. A high expression level of OSM is related to poor outcomes in breast cancer [83] and the promotion of breast cancer metastasis [84, 85]. AVPR1B is one of the receptors of Arginine vasopressin and positively correlated with the

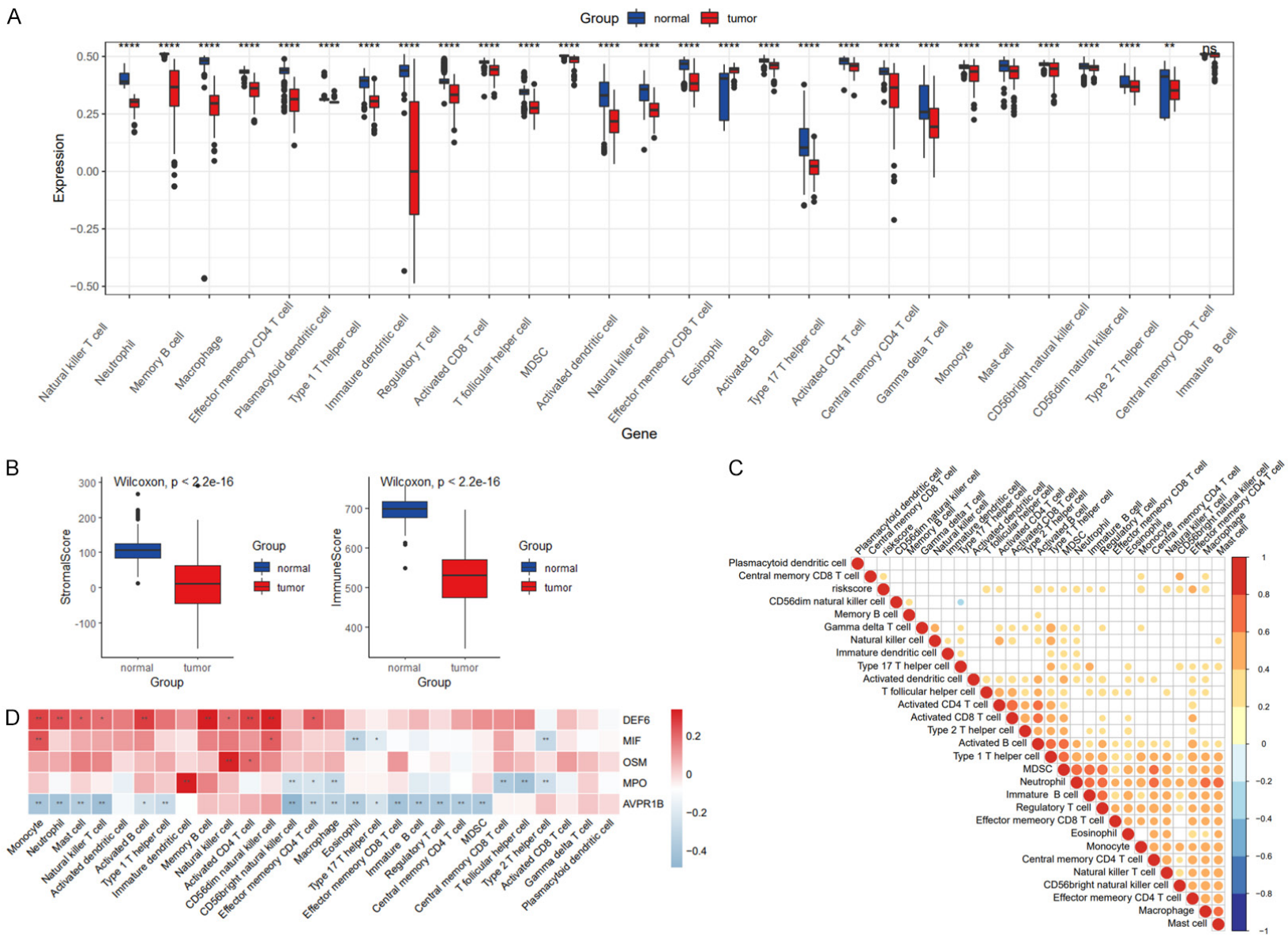

Figure 8. Evaluation of immune cell infiltration in AML tumor microenvironment. A. Boxplot of immune cell abundance between normal and AML samples; B. Using estimation algorithm to calculate immunity score and stromal score between normal and AML samples; C. The correlation between risk score and immune cells infiltration in non-M3 AML patients; D. The correlation between immune cells and 5 IRGs (*P < 0.05, **P < 0.01, ***P < 0.001).

elevation of plasma adrenocorticotropin in corticotropinomas [86], the specific AVPR1B agonists could be used for rapid correction of anemia after bleeding, drug toxicity, or chemotherapy [87]. It is important to elucidate the functions of AVPR1B, DEF6 and OSM in AML in future studies. Since MIF and DEF6 are overexpressed in AML and positively correlated with AML prognosis, those two molecular might be used as diagnostic markers and therapeutic targets.

The success of 5-gene model in prediction of AML prognosis indicated the functions of those 5 genes in AML progression and/or treatment response. In a view to immunosuppression functions of those 5 genes, MIF promoted the polarization of M2-TAMs, which were critical immunosuppressive cells [88, 89]. Moreover, previous studies demonstrated that MIF bond to macrophage receptor CD74 and activated the ERK pathway within cells, a pathway that promoted tumor cell proliferation [90, 91]. Additionally, MIF was able to inhibit NK cell activity by downregulating NKG2D receptors and promoted ovarian cancer immune escape [92, 93]. MPO is a marker for distinguishing myeloid or lymphoid leukemia, but its role in immune escape is not clear [94]. The immunosuppressive functions of OSM, DEF6 and AVPR1B have yet been recognized. Previous studies demonstrated that the immunosuppressive microenvironment of AML was related to the increase of Tregs and MDSCs in the peripheral blood and bone marrow (BM) [57]. Tregs promoted the expansion and recurrence of AML blasts by secreting immunosuppressive cytokines and increasing ATP hydrolysis [21, 95]. Moreover, by expressing ectonucleotides CD73 and CD39, leukemia cells could produce adenosine, thereby suppressing the function of effector T cells and promoting Tregs [96]. The number of Tregs was negatively correlated with the prognosis of patients [57]. In MDSCs research, previous studies shown that AML tumor cells mimicked MDSCs in suppressing anti-AML T cell responses [97, 98]. Specifically, AML tumor cells could induce T cells and NK cells apoptosis via ROS [97, 99]. Alternatively, AML tumor cells also regulated arginine metabolism in T cells and inhibit cytotoxic lymphocytes via tryptophan metabolism [100-102]. At last, direct contact between NK cells and tumor cells could also lead to dysfunction of NK cells [103, 104]. Overall, our findings from ssGSEA analysis agreed with those bench data.

As a conclusion, we developed an immune gene expression model to predict the outcome of AML patients. There were several limitations of this study. First, the model was only validated by clinical informatics data. A multicenter clinical study might provide further validation of the prediction model. Second, the infiltration of immune cells in AML TME was not validated. AML patient BM aspiration samples could be used for immune cells counting to validate our result from bioinformatics analysis. Third, mechanisms underline 5-gene prediction model, as well as characteristic immune cells infiltration in AML TME, were not addressed in this study. In particular, the immunosuppression functions of identified 5 genes in AML might provide great insight to AML therapy.

Acknowledgements

Thanks to Dr. Jianming Zeng (University of Macau) and all members of his bioinformatics team, biotrainee, for graciously sharing their codes and experience. The research was supported in part by grants to Y.Z. from the Sichuan University Faculty Start Fund, as well as the National Science Foundation of China (Nos. 81870157 and 82070219).

Disclosure of conflict of interest

None.

Address correspondence to: Drs. Yuhuan Zheng and Ting Niu, Department of Hematology, West China Hospital, and State Key Laboratory of Biotherapy and Cancer Center, Sichuan University, #37 Guo Xue Xiang Street, Chengdu 610041, China. Tel: 86-28-85403107; E-mail: zhengyuhuan@scu.edu.cn (YHZ); Tel: 86-28-85403107; E-mail: tingniu@sina.com.cn (TN)

References

[1] Döhner H, Weisdorf DJ and Bloomfield CD. Acute myeloid leukemia. N Engl J Med 2015; 373: 1136-1152.
[2] De Kouchkovsky I and Abdul-Hay M. 'Acute myeloid leukemia: a comprehensive review and 2016 update'. Blood Cancer J 2016; 6: e441.
[3] Coombs CC, Tavakkoli M and Tallman MS. Acute promyelocytic leukemia: where did we

start, where are we now, and the future. Blood Cancer J 2015; 5: e304.
[4] Shen ZX, Shi ZZ, Fang J, Gu BW, Li JM, Zhu YM, Shi JY, Zheng PZ, Yan H, Liu YF, Chen Y, Shen Y, Wu W, Tang W, Waxman S, De Thé H, Wang ZY, Chen SJ and Chen Z. All-trans retinoic acid/As2O3 combination yields a high quality remission and survival in newly diagnosed acute promyelocytic leukemia. Proc Natl Acad Sci U S A 2004; 101: 5328-5335.
[5] Döhner H, Estey EH, Amadori S, Appelbaum FR, Büchner T, Burnett AK, Dombret H, Fenaux P, Grimwade D, Larson RA, Lo-Coco F, Naoe T, Niederwieser D, Ossenkoppele GJ, Sanz MA, Sierra J, Tallman MS, Löwenberg B and Bloomfield CD. Diagnosis and management of acute myeloid leukemia in adults: recommendations from an international expert panel, on behalf of the European LeukemiaNet. Blood 2010; 115: 453-474.
[6] Martínez-Sánchez MV, Fuster JL, Campillo JA, Galera AM, Bermúdez-Cortés M, Llinares ME, Ramos-Elbal E, Pascual-Gázquez JF, Fita AM, Martínez-Banaclocha H, Galián JA, Gimeno L, Muro M and Minguela A. Expression of NK cell receptor ligands on leukemic cells is associated with the outcome of childhood acute leukemia. Cancers (Basel) 2021; 13: 2294.
[7] Zhang J, Hu X, Wang J, Sahu AD, Cohen D, Song L, Ouyang Z, Fan J, Wang B, Fu J, Gu S, Sade-Feldman M, Hacohen N, Li W, Ying X, Li B and Liu XS. Immune receptor repertoires in pediatric and adult acute myeloid leukemia. Genome Med 2019; 11: 73.
[8] Liu G, Zhang Q, Yang J, Li X, Xian L, Li W, Lin T, Cheng J, Lin Q, Xu X, Li Q, Lin Y, Zhou M and Shen E. Increased TIGIT expressing NK cells with dysfunctional phenotype in AML patients correlated with poor prognosis. Cancer Immunol Immunother 2022; 71: 277-287.
[9] Yu G, Wang LG, Han Y and He QY. ClusterProfiler: an R package for comparing biological themes among gene clusters. Omics 2012; 16: 284-287.
[10] Zhang Y, Ma S, Wang M, Shi W and Hu Y. Comprehensive analysis of prognostic markers for acute myeloid leukemia based on four metabolic genes. Front Oncol 2020; 10: 578933.
[11] Charoentong P, Finotello F, Angelova M, Mayer C, Efremova M, Rieder D, Hackl H and Trajanoski Z. Pan-cancer immunogenomic analyses reveal genotype-immunophenotype relationships and predictors of response to checkpoint blockade. Cell Rep 2017; 18: 248-262.
[12] Barbie DA, Tamayo P, Boehm JS, Kim SY, Moody SE, Dunn IF, Schinzel AC, Sandy P, Meylan E, Scholl C, Fröhling S, Chan EM, Sos ML, Michel K, Mermel C, Silver SJ, Weir BA, Reiling JH, Sheng Q, Gupta PB, Wadlow RC, Le H, Hoersch S, Wittner BS, Ramaswamy S, Livingston DM, Sabatini DM, Meyerson M, Thomas RK, Lander ES, Mesirov JP, Root DE, Gilliland DG, Jacks T and Hahn WC. Systematic RNA interference reveals that oncogenic KRAS-driven cancers require TBK1. Nature 2009; 462: 108-112.
[13] Calin GA, Ferracin M, Cimmino A, Di Leva G, Shimizu M, Wojcik SE, Iorio MV, Visone R, Sever NI, Fabbri M, Iuliano R, Palumbo T, Pichiorri F, Roldo C, Garzon R, Sevignani C, Rassenti L, Alder H, Volinia S, Liu CG, Kipps TJ, Negrini M and Croce CM. A microRNA signature associated with prognosis and progression in chronic lymphocytic leukemia. N Engl J Med 2005; 353: 1793-1801.
[14] Li X, Zhang Y, Zhang Y, Ding J, Wu K and Fan D. Survival prediction of gastric cancer by a seven-microRNA signature. Gut 2010; 59: 579-585.
[15] Bhattacharya S, Dunn P, Thomas CG, Smith B, Schaefer H, Chen J, Hu Z, Zalocusky KA, Shankar RD, Shen-Orr SS, Thomson E, Wiser J and Butte AJ. ImmPort, toward repurposing of open access immunological assay data for translational and clinical research. Sci Data 2018; 5: 180015.
[16] Ustun C, Miller JS, Munn DH, Weisdorf DJ and Blazar BR. Regulatory T cells in acute myelogenous leukemia: is it time for immunomodulation? Blood 2011; 118: 5084-5095.
[17] Pyzer AR, Stroopinsky D, Rajabi H, Washington A, Tagde A, Coll M, Fung J, Bryant MP, Cole L, Palmer K, Somaiya P, Karp Leaf R, Nahas M, Apel A, Jain S, McMasters M, Mendez L, Levine J, Joyce R, Arnason J, Pandolfi PP, Kufe D, Rosenblatt J and Avigan D. MUC1-mediated induction of myeloid-derived suppressor cells in patients with acute myeloid leukemia. Blood 2017; 129: 1791-1801.
[18] Mantovani A, Sozzani S, Locati M, Allavena P and Sica A. Macrophage polarization: tumor-associated macrophages as a paradigm for polarized M2 mononuclear phagocytes. Trends Immunol 2002; 23: 549-555.
[19] Al-Matary YS, Botezatu L, Opalka B, Hönes JM, Lams RF, Thivakaran A, Schütte J, Köster R, Lennartz K, Schroeder T, Haas R, Dührsen U and Khandanpour C. Acute myeloid leukemia cells polarize macrophages towards a leukemia supporting state in a Growth factor independence 1 dependent manner. Haematologica 2016; 101: 1216-1227.
[20] Tie Y, Tang F, Wei YQ and Wei XW. Immunosuppressive cells in cancer: mechanisms and potential therapeutic targets. J Hematol Oncol 2022; 15: 61.
[21] Szczepanski MJ, Szajnik M, Czystowska M, Mandapathil M, Strauss L, Welsh A, Foon KA, Whiteside TL and Boyiadzis M. Increased fre-

quency and suppression by regulatory T cells in patients with acute myelogenous leukemia. Clin Cancer Res 2009; 15: 3325-3332.
[22] Toomer KH and Malek TR. Cytokine signaling in the development and homeostasis of regulatory T cells. Cold Spring Harb Perspect Biol 2018; 10: a028597.
[23] Ghiringhelli F, Ménard C, Terme M, Flament C, Taieb J, Chaput N, Puig PE, Novault S, Escudier B, Vivier E, Lecesne A, Robert C, Blay JY, Bernard J, Caillat-Zucman S, Freitas A, Tursz T, Wagner-Ballon O, Capron C, Vainchencker W, Martin F and Zitvogel L. CD4+CD25+ regulatory T cells inhibit natural killer cell functions in a transforming growth factor-beta-dependent manner. J Exp Med 2005; 202: 1075-1085.
[24] Szczepanski MJ, Szajnik M, Welsh A, Whiteside TL and Boyiadzis M. Blast-derived microvesicles in sera from patients with acute myeloid leukemia suppress natural killer cell function via membrane-associated transforming growth factor-beta1. Haematologica 2011; 96: 1302-1309.
[25] Budhu S, Schaer DA, Li Y, Toledo-Crow R, Panageas K, Yang X, Zhong H, Houghton AN, Silverstein SC, Merghoub T and Wolchok JD. Blockade of surface-bound TGF-β on regulatory T cells abrogates suppression of effector T cell function in the tumor microenvironment. Sci Signal 2017; 10: eaak9702.
[26] Knochelmann HM, Dwyer CJ, Bailey SR, Amaya SM, Elston DM, Mazza-McCrann JM and Paulos CM. When worlds collide: Th17 and Treg cells in cancer and autoimmunity. Cell Mol Immunol 2018; 15: 458-469.
[27] Folgiero V, Cifaldi L, Li Pira G, Goffredo BM, Vinti L and Locatelli F. TIM-3/Gal-9 interaction induces IFNγ-dependent IDO1 expression in acute myeloid leukemia blast cells. J Hematol Oncol 2015; 8: 36.
[28] Curti A, Pandolfi S, Valzasina B, Aluigi M, Isidori A, Ferri E, Salvestrini V, Bonanno G, Rutella S, Durelli I, Horenstein AL, Fiore F, Massaia M, Colombo MP, Baccarani M and Lemoli RM. Modulation of tryptophan catabolism by human leukemic cells results in the conversion of CD25- into CD25+ T regulatory cells. Blood 2007; 109: 2871-2877.
[29] Yoyen-Ermis D, Tunali G, Tavukcuoglu E, Horzum U, Ozkazanc D, Sutlu T, Buyukasik Y and Esendagli G. Myeloid maturation potentiates STAT3-mediated atypical IFN-γ signaling and upregulation of PD-1 ligands in AML and MDS. Sci Rep 2019; 9: 11697.
[30] Krönig H, Kremmler L, Haller B, Englert C, Peschel C, Andreesen R and Blank CU. Interferon-induced programmed death-ligand 1 (PD-L1/B7-H1) expression increases on human acute myeloid leukemia blast cells during treatment. Eur J Haematol 2014; 92: 195-203.
[31] Berthon C, Driss V, Liu J, Kuranda K, Leleu X, Jouy N, Hetuin D and Quesnel B. In acute myeloid leukemia, B7-H1 (PD-L1) protection of blasts from cytotoxic T cells is induced by TLR ligands and interferon-gamma and can be reversed using MEK inhibitors. Cancer Immunol Immunother 2010; 59: 1839-1849.
[32] Norde WJ, Maas F, Hobo W, Korman A, Quigley M, Kester MG, Hebeda K, Falkenburg JH, Schaap N, de Witte TM, van der Voort R and Dolstra H. PD-1/PD-L1 interactions contribute to functional T-cell impairment in patients who relapse with cancer after allogeneic stem cell transplantation. Cancer Res 2011; 71: 5111-5122.
[33] Taki M, Abiko K, Baba T, Hamanishi J, Yamaguchi K, Murakami R, Yamanoi K, Horikawa N, Hosoe Y, Nakamura E, Sugiyama A, Mandai M, Konishi I and Matsumura N. Snail promotes ovarian cancer progression by recruiting myeloid-derived suppressor cells via CXCR2 ligand upregulation. Nat Commun 2018; 9: 1685.
[34] Chao T, Furth EE and Vonderheide RH. CXCR2-dependent accumulation of tumor-associated neutrophils regulates T-cell immunity in pancreatic ductal adenocarcinoma. Cancer Immunol Res 2016; 4: 968-982.
[35] Saleh R and Elkord E. Acquired resistance to cancer immunotherapy: role of tumor-mediated immunosuppression. Semin Cancer Biol 2020; 65: 13-27.
[36] Pedroza-Gonzalez A, Zhou G, Vargas-Mendez E, Boor PP, Mancham S, Verhoef C, Polak WG, Grünhagen D, Pan Q, Janssen H, Garcia-Romo GS, Biermann K, Tjwa ET, JN IJ, Kwekkeboom J and Sprengers D. Tumor-infiltrating plasmacytoid dendritic cells promote immunosuppression by Tr1 cells in human liver tumors. Oncoimmunology 2015; 4: e1008355.
[37] Gabrilovich DI, Ostrand-Rosenberg S and Bronte V. Coordinated regulation of myeloid cells by tumours. Nat Rev Immunol 2012; 12: 253-268.
[38] Fridlender ZG, Sun J, Kim S, Kapoor V, Cheng G, Ling L, Worthen GS and Albelda SM. Polarization of tumor-associated neutrophil phenotype by TGF-beta: "N1" versus "N2" TAN. Cancer Cell 2009; 16: 183-194.
[39] Jaillon S, Ponzetta A, Di Mitri D, Santoni A, Bonecchi R and Mantovani A. Neutrophil diversity and plasticity in tumour progression and therapy. Nat Rev Cancer 2020; 20: 485-503.
[40] Nozawa H, Chiu C and Hanahan D. Infiltrating neutrophils mediate the initial angiogenic switch in a mouse model of multistage carci-

nogenesis. Proc Natl Acad Sci U S A 2006; 103: 12493-12498.
[41] Schauer C, Janko C, Munoz LE, Zhao Y, Kienhöfer D, Frey B, Lell M, Manger B, Rech J, Naschberger E, Holmdahl R, Krenn V, Harrer T, Jeremic I, Bilyy R, Schett G, Hoffmann M and Herrmann M. Aggregated neutrophil extracellular traps limit inflammation by degrading cytokines and chemokines. Nat Med 2014; 20: 511-517.
[42] Demers M, Wong SL, Martinod K, Gallant M, Cabral JE, Wang Y and Wagner DD. Priming of neutrophils toward NETosis promotes tumor growth. Oncoimmunology 2016; 5: e1134073.
[43] Cheng N, Bai X, Shu Y, Ahmad O and Shen P. Targeting tumor-associated macrophages as an antitumor strategy. Biochem Pharmacol 2021; 183: 114354.
[44] Ngambenjawong C, Gustafson HH and Pun SH. Progress in tumor-associated macrophage (TAM)-targeted therapeutics. Adv Drug Deliv Rev 2017; 114: 206-221.
[45] Yoshihara K, Shahmoradgoli M, Martínez E, Vegesna R, Kim H, Torres-Garcia W, Treviño V, Shen H, Laird PW, Levine DA, Carter SL, Getz G, Stemke-Hale K, Mills GB and Verhaak RG. Inferring tumour purity and stromal and immune cell admixture from expression data. Nat Commun 2013; 4: 2612.
[46] Robert C, Long GV, Brady B, Dutriaux C, Maio M, Mortier L, Hassel JC, Rutkowski P, McNeil C, Kalinka-Warzocha E, Savage KJ, Hernberg MM, Lebbé C, Charles J, Mihalcioiu C, Chiarion-Sileni V, Mauch C, Cognetti F, Arance A, Schmidt H, Schadendorf D, Gogas H, Lundgren-Eriksson L, Horak C, Sharkey B, Waxman IM, Atkinson V and Ascierto PA. Nivolumab in previously untreated melanoma without BRAF mutation. N Engl J Med 2015; 372: 320-330.
[47] Freeman-Keller M, Goldman J and Gray J. Vaccine immunotherapy in lung cancer: clinical experience and future directions. Pharmacol Ther 2015; 153: 1-9.
[48] Motzer RJ, Tannir NM, McDermott DF, Arén Frontera O, Melichar B, Choueiri TK, Plimack ER, Barthélémy P, Porta C, George S, Powles T, Donskov F, Neiman V, Kollmannsberger CK, Salman P, Gurney H, Hawkins R, Ravaud A, Grimm MO, Bracarda S, Barrios CH, Tomita Y, Castellano D, Rini BI, Chen AC, Mekan S, McHenry MB, Wind-Rotolo M, Doan J, Sharma P, Hammers HJ and Escudier B. Nivolumab plus Ipilimumab versus sunitinib in advanced renal-cell carcinoma. N Engl J Med 2018; 378: 1277-1290.
[49] Koreth J, Schlenk R, Kopecky KJ, Honda S, Sierra J, Djulbegovic BJ, Wadleigh M, DeAngelo DJ, Stone RM, Sakamaki H, Appelbaum FR, Döhner H, Antin JH, Soiffer RJ and Cutler C. Allogeneic stem cell transplantation for acute myeloid leukemia in first complete remission: systematic review and meta-analysis of prospective clinical trials. JAMA 2009; 301: 2349-2361.
[50] Amadori S, Suciu S, Selleslag D, Aversa F, Gaidano G, Musso M, Annino L, Venditti A, Voso MT, Mazzone C, Magro D, De Fabritiis P, Muus P, Alimena G, Mancini M, Hagemeijer A, Paoloni F, Vignetti M, Fazi P, Meert L, Ramadan SM, Willemze R, de Witte T and Baron F. Gemtuzumab ozogamicin versus best supportive care in older patients with newly diagnosed acute myeloid leukemia unsuitable for intensive chemotherapy: results of the randomized phase III EORTC-GIMEMA AML-19 trial. J Clin Oncol 2016; 34: 972-979.
[51] Burnett AK, Russell NH, Hills RK, Kell J, Freeman S, Kjeldsen L, Hunter AE, Yin J, Craddock CF, Dufva IH, Wheatley K and Milligan D. Addition of gemtuzumab ozogamicin to induction chemotherapy improves survival in older patients with acute myeloid leukemia. J Clin Oncol 2012; 30: 3924-3931.
[52] Tamamyan G, Kadia T, Ravandi F, Borthakur G, Cortes J, Jabbour E, Daver N, Ohanian M, Kantarjian H and Konopleva M. Frontline treatment of acute myeloid leukemia in adults. Crit Rev Oncol Hematol 2017; 110: 20-34.
[53] Austin R, Smyth MJ and Lane SW. Harnessing the immune system in acute myeloid leukaemia. Crit Rev Oncol Hematol 2016; 103: 62-77.
[54] Daver N, Boddu P, Garcia-Manero G, Yadav SS, Sharma P, Allison J and Kantarjian H. Hypomethylating agents in combination with immune checkpoint inhibitors in acute myeloid leukemia and myelodysplastic syndromes. Leukemia 2018; 32: 1094-1105.
[55] Kayser S and Levis MJ. Advances in targeted therapy for acute myeloid leukaemia. Br J Haematol 2018; 180: 484-500.
[56] Qasim W. Allogeneic CAR T cell therapies for leukemia. Am J Hematol 2019; 94: S50-S54.
[57] Beyar-Katz O and Gill S. Novel approaches to acute myeloid leukemia immunotherapy. Clin Cancer Res 2018; 24: 5502-5515.
[58] Döhner H, Estey E, Grimwade D, Amadori S, Appelbaum FR, Büchner T, Dombret H, Ebert BL, Fenaux P, Larson RA, Levine RL, Lo-Coco F, Naoe T, Niederwieser D, Ossenkoppele GJ, Sanz M, Sierra J, Tallman MS, Tien HF, Wei AH, Löwenberg B and Bloomfield CD. Diagnosis and management of AML in adults: 2017 ELN recommendations from an international expert panel. Blood 2017; 129: 424-447.
[59] Grimm J, Jentzsch M, Bill M, Goldmann K, Schulz J, Niederwieser D, Platzbecker U and Schwind S. Prognostic impact of the ELN2017 risk classification in patients with AML receiving allogeneic transplantation. Blood Adv 2020; 4: 3864-3874.

[60] Chantepie SP, Parienti JJ, Salaun V, Benabed K, Cheze S, Gac AC, Johnson-Ansah H, Macro M, Damaj G, Vilque JP and Reman O. The prognostic value of hematogones in patients with acute myeloid leukemia. Am J Hematol 2016; 91: 566-570.
[61] Wang JD, Zhou HS, Tu XX, He Y, Liu QF, Liu Q and Long ZJ. Prediction of competing endogenous RNA coexpression network as prognostic markers in AML. Aging (Albany NY) 2019; 11: 3333-3347.
[62] Wilop S, Chou WC, Jost E, Crysandt M, Panse J, Chuang MK, Brümmendorf TH, Wagner W, Tien HF and Kharabi Masouleh B. A three-gene expression-based risk score can refine the European LeukemiaNet AML classification. J Hematol Oncol 2016; 9: 78.
[63] Zhu R, Tao H, Lin W, Tang L and Hu Y. Identification of an immune-related gene signature based on immunogenomic landscape analysis to predict the prognosis of adult acute myeloid leukemia patients. Front Oncol 2020; 10: 574939.
[64] Li R, Ding Z, Jin P, Wu S, Jiang G, Xiang R, Wang W, Jin Z, Li X, Xue K, Wu X and Li J. Development and validation of a novel prognostic model for acute myeloid leukemia based on immune-related genes. Front Immunol 2021; 12: 639634.
[65] Bernhagen J, Krohn R, Lue H, Gregory JL, Zernecke A, Koenen RR, Dewor M, Georgiev I, Schober A, Leng L, Kooistra T, Fingerle-Rowson G, Ghezzi P, Kleemann R, McColl SR, Bucala R, Hickey MJ and Weber C. MIF is a noncognate ligand of CXC chemokine receptors in inflammatory and atherogenic cell recruitment. Nat Med 2007; 13: 587-596.
[66] Simons D, Grieb G, Hristov M, Pallua N, Weber C, Bernhagen J and Steffens G. Hypoxia-induced endothelial secretion of macrophage migration inhibitory factor and role in endothelial progenitor cell recruitment. J Cell Mol Med 2011; 15: 668-678.
[67] Falantes JF, Trujillo P, Piruat JI, Calderón C, Márquez-Malaver FJ, Martín-Antonio B, Millán A, Gómez M, González J, Martino ML, Montero I, Parody R, Espigado I, Urbano-Ispizua A and Pérez-Simón JA. Overexpression of GYS1, MIF, and MYC is associated with adverse outcome and poor response to azacitidine in myelodysplastic syndromes and acute myeloid leukemia. Clin Lymphoma Myeloma Leuk 2015; 15: 236-244.
[68] Abdul-Aziz AM, Shafat MS, Mehta TK, Di Palma F, Lawes MJ, Rushworth SA and Bowles KM. MIF-Induced stromal PKCβ/IL8 is essential in human acute myeloid leukemia. Cancer Res 2017; 77: 303-311.
[69] Abdul-Aziz AM, Shafat MS, Sun Y, Marlein CR, Piddock RE, Robinson SD, Edwards DR, Zhou Z, Collins A, Bowles KM and Rushworth SA. HIF1α drives chemokine factor pro-tumoral signaling pathways in acute myeloid leukemia. Oncogene 2018; 37: 2676-2686.
[70] Kamijo R, Itonaga H, Kihara R, Nagata Y, Hata T, Asou N, Ohtake S, Shiraishi Y, Chiba K, Tanaka H, Miyano S, Ogawa S, Naoe T, Kiyoi H and Miyazaki Y. Distinct gene alterations with a high percentage of myeloperoxidase-positive leukemic blasts in de novo acute myeloid leukemia. Leuk Res 2018; 65: 34-41.
[71] Sawayama Y, Miyazaki Y, Ando K, Horio K, Tsutsumi C, Imanishi D, Tsushima H, Imaizumi Y, Hata T, Fukushima T, Yoshida S, Onimaru Y, Iwanaga M, Taguchi J, Kuriyama K and Tomonaga M. Expression of myeloperoxidase enhances the chemosensitivity of leukemia cells through the generation of reactive oxygen species and the nitration of protein. Leukemia 2008; 22: 956-964.
[72] Itonaga H, Imanishi D, Wong YF, Sato S, Ando K, Sawayama Y, Sasaki D, Tsuruda K, Hasegawa H, Imaizumi Y, Taguchi J, Tsushima H, Yoshida S, Fukushima T, Hata T, Moriuchi Y, Yanagihara K and Miyazaki Y. Expression of myeloperoxidase in acute myeloid leukemia blasts mirrors the distinct DNA methylation pattern involving the downregulation of DNA methyltransferase DNMT3B. Leukemia 2014; 28: 1459-1466.
[73] Matsuo T, Kuriyama K, Miyazaki Y, Yoshida S, Tomonaga M, Emi N, Kobayashi T, Miyawaki S, Matsushima T, Shinagawa K, Honda S and Ohno R. The percentage of myeloperoxidase-positive blast cells is a strong independent prognostic factor in acute myeloid leukemia, even in the patients with normal karyotype. Leukemia 2003; 17: 1538-1543.
[74] Gupta S, Fanzo JC, Hu C, Cox D, Jang SY, Lee AE, Greenberg S and Pernis AB. T cell receptor engagement leads to the recruitment of IBP, a novel guanine nucleotide exchange factor, to the immunological synapse. J Biol Chem 2003; 278: 43541-43549.
[75] Samson T, Will C, Knoblauch A, Sharek L, von der Mark K, Burridge K and Wixler V. Def-6, a guanine nucleotide exchange factor for Rac1, interacts with the skeletal muscle integrin chain alpha7A and influences myoblast differentiation. J Biol Chem 2007; 282: 15730-15742.
[76] Liew PL, Fang CY, Lee YC, Lee YC, Chen CL and Chu JS. DEF6 expression in ovarian carcinoma correlates with poor patient survival. Diagn Pathol 2016; 11: 68.
[77] Zhang Q, Zhao GS, Cao Y, Tang XF, Tan QL, Lin L and Guo QN. Increased DEF6 expression is correlated with metastasis and poor prognosis in human osteosarcoma. Oncol Lett 2020; 20: 1629-1640.

[78] Zhu ZP, Lin LR, Lv TD, Xu CR, Cai TY and Lin J. High expression levels of DEF6 predicts a poor prognosis for patients with clear cell renal cell carcinoma. Oncol Rep 2020; 44: 2056-2066.
[79] Lu C, Rak JW, Kobayashi H and Kerbel RS. Increased resistance to oncostatin M-induced growth inhibition of human melanoma cell lines derived from advanced-stage lesions. Cancer Res 1993; 53: 2708-2711.
[80] Tanaka M and Miyajima A. Oncostatin M, a multifunctional cytokine. Rev Physiol Biochem Pharmacol 2003; 149: 39-52.
[81] Grant SL and Begley CG. The oncostatin M signalling pathway: reversing the neoplastic phenotype? Mol Med Today 1999; 5: 406-412.
[82] Jones SA and Jenkins BJ. Recent insights into targeting the IL-6 cytokine family in inflammatory diseases and cancer. Nat Rev Immunol 2018; 18: 773-789.
[83] West NR, Murphy LC and Watson PH. Oncostatin M suppresses oestrogen receptor-α expression and is associated with poor outcome in human breast cancer. Endocr Relat Cancer 2012; 19: 181-195.
[84] Tawara K, Bolin C, Koncinsky J, Kadaba S, Covert H, Sutherland C, Bond L, Kronz J, Garbow JR and Jorcyk CL. OSM potentiates preintravasation events, increases CTC counts, and promotes breast cancer metastasis to the lung. Breast Cancer Res 2018; 20: 53.
[85] West NR, Murray JI and Watson PH. Oncostatin-M promotes phenotypic changes associated with mesenchymal and stem cell-like differentiation in breast cancer. Oncogene 2014; 33: 1485-1494.
[86] Luque RM, Ibáñez-Costa A, López-Sánchez LM, Jiménez-Reina L, Venegas-Moreno E, Gálvez MA, Villa-Osaba A, Madrazo-Atutxa AM, Japón MA, de la Riva A, Cano DA, Benito-López P, Soto-Moreno A, Gahete MD, Leal-Cerro A and Castaño JP. A cellular and molecular basis for the selective desmopressin-induced ACTH release in Cushing disease patients: key role of AVPR1b receptor and potential therapeutic implications. J Clin Endocrinol Metab 2013; 98: 4160-4169.
[87] Mayer B, Németh K, Krepuska M, Myneni VD, Maric D, Tisdale JF, Hsieh MM, Uchida N, Lee HJ, Nemeth MJ, Holmbeck K, Noguchi CT, Rogers H, Dey S, Hansen A, Hong J, Chow I, Key S, Szalayova I, Pagani J, Markó K, McClain-Caldwell I, Vitale-Cross L, Young WS, Brownstein MJ and Mezey É. Vasopressin stimulates the proliferation and differentiation of red blood cell precursors and improves recovery from anemia. Sci Transl Med 2017; 9: eaao1632.
[88] Noe JT and Mitchell RA. MIF-dependent control of tumor immunity. Front Immunol 2020; 11: 609948.
[89] Yaddanapudi K, Putty K, Rendon BE, Lamont GJ, Faughn JD, Satoskar A, Lasnik A, Eaton JW and Mitchell RA. Control of tumor-associated macrophage alternative activation by macrophage migration inhibitory factor. J Immunol 2013; 190: 2984-2993.
[90] Leng L, Metz CN, Fang Y, Xu J, Donnelly S, Baugh J, Delohery T, Chen Y, Mitchell RA and Bucala R. MIF signal transduction initiated by binding to CD74. J Exp Med 2003; 197: 1467-1476.
[91] Shi X, Leng L, Wang T, Wang W, Du X, Li J, McDonald C, Chen Z, Murphy JW, Lolis E, Noble P, Knudson W and Bucala R. CD44 is the signaling component of the macrophage migration inhibitory factor-CD74 receptor complex. Immunity 2006; 25: 595-606.
[92] Bauer S, Groh V, Wu J, Steinle A, Phillips JH, Lanier LL and Spies T. Activation of NK cells and T cells by NKG2D, a receptor for stress-inducible MICA. Science 1999; 285: 727-729.
[93] Calandra T and Roger T. Macrophage migration inhibitory factor: a regulator of innate immunity. Nat Rev Immunol 2003; 3: 791-800.
[94] Bras AE, Osmani Z, de Haas V, Jongen-Lavrencic M, Te Marvelde JG, Zwaan CM, Mejstrikova E, Fernandez P, Szczepanski T, Orfao A, van Dongen JJM and van der Velden VHJ. Standardised immunophenotypic analysis of myeloperoxidase in acute leukaemia. Br J Haematol 2021; 193: 922-927.
[95] Shenghui Z, Yixiang H, Jianbo W, Kang Y, Laixi B, Yan Z and Xi X. Elevated frequencies of $CD4^+$ $CD25^+$ CD127lo regulatory T cells is associated to poor prognosis in patients with acute myeloid leukemia. Int J Cancer 2011; 129: 1373-1381.
[96] Dulphy N, Henry G, Hemon P, Khaznadar Z, Dombret H, Boissel N, Bensussan A and Toubert A. Contribution of CD39 to the immunosuppressive microenvironment of acute myeloid leukaemia at diagnosis. Br J Haematol 2014; 165: 722-725.
[97] Aurelius J, Thorén FB, Akhiani AA, Brune M, Palmqvist L, Hansson M, Hellstrand K and Martner A. Monocytic AML cells inactivate antileukemic lymphocytes: role of NADPH oxidase/gp91 (phox) expression and the PARP-1/PAR pathway of apoptosis. Blood 2012; 119: 5832-5837.
[98] Mehta RS, Chen X, Antony J, Boyiadzis M and Szabolcs P. Generating peripheral blood derived lymphocytes reacting against autologous primary AML blasts. J Immunother 2016; 39: 71-80.
[99] Zhou F, Shen Q and Claret FX. Novel roles of reactive oxygen species in the pathogenesis of acute myeloid leukemia. J Leukoc Biol 2013; 94: 423-429.

[100] Mussai F, De Santo C, Abu-Dayyeh I, Booth S, Quek L, McEwen-Smith RM, Qureshi A, Dazzi F, Vyas P and Cerundolo V. Acute myeloid leukemia creates an arginase-dependent immunosuppressive microenvironment. Blood 2013; 122: 749-758.
[101] Della Chiesa M, Carlomagno S, Frumento G, Balsamo M, Cantoni C, Conte R, Moretta L, Moretta A and Vitale M. The tryptophan catabolite L-kynurenine inhibits the surface expression of NKp46- and NKG2D-activating receptors and regulates NK-cell function. Blood 2006; 108: 4118-4125.
[102] Curti A, Aluigi M, Pandolfi S, Ferri E, Isidori A, Salvestrini V, Durelli I, Horenstein AL, Fiore F, Massaia M, Piccioli M, Pileri SA, Zavatto E, D'Addio A, Baccarani M and Lemoli RM. Acute myeloid leukemia cells constitutively express the immunoregulatory enzyme indoleamine 2,3-dioxygenase. Leukemia 2007; 21: 353-355.
[103] Orleans-Lindsay JK, Barber LD, Prentice HG and Lowdell MW. Acute myeloid leukaemia cells secrete a soluble factor that inhibits T and NK cell proliferation but not cytolytic function--implications for the adoptive immunotherapy of leukaemia. Clin Exp Immunol 2001; 126: 403-411.
[104] Fauriat C, Just-Landi S, Mallet F, Arnoulet C, Sainty D, Olive D and Costello RT. Deficient expression of NCR in NK cells from acute myeloid leukemia: evolution during leukemia treatment and impact of leukemia cells in NCR-dull phenotype induction. Blood 2007; 109: 323-330.

Table S1. Intersection of DEGs and IRGs

gene_name	Row.names	*P* Value	FDR	gene_type	ENTREZID
A2M-AS1	ENSG00000245105.2	1.62E-46	4.46E-46	antisense	144571
ADARB2-AS1	ENSG00000205696.4	1.27E-43	3.39E-43	antisense	642394
ADH5P4	ENSG00000233859.2	2.54E-39	6.46E-39	processed_pseudogene	642443
ADIPOR1P2	ENSG00000258805.1	6.58E-31	1.51E-30	processed_pseudogene	390503
ADM2	ENSG00000128165.8	3.36E-21	6.67E-21	protein_coding	79924
ADRB1	ENSG00000043591.5	3.07E-41	7.96E-41	protein_coding	153
AGRP	ENSG00000159723.4	8.03E-158	5.52E-157	protein_coding	181
AGT	ENSG00000135744.7	0.85405849	0.86616466	protein_coding	183
AHNAK2	ENSG00000185567.6	1.58E-45	4.31E-45	protein_coding	113146
AIMP1P1	ENSG00000234187.1	1.37E-36	3.37E-36	processed_pseudogene	170547
AKT3-IT1	ENSG00000228939.1	6.56E-104	3.03E-103	sense_intronic	100874263
AMH	ENSG00000104899.5	3.40E-27	7.39E-27	protein_coding	268
ANGPT4	ENSG00000101280.7	3.95E-26	8.47E-26	protein_coding	51378
ANGPTL7	ENSG00000171819.4	3.08E-66	1.03E-65	protein_coding	10218
APCS	ENSG00000132703.3	2.03E-49	5.74E-49	protein_coding	325
APLNR	ENSG00000134817.10	2.95E-11	4.83E-11	protein_coding	187
ARAP1-AS1	ENSG00000256007.1	2.42E-29	5.43E-29	antisense	100874075
ART1	ENSG00000129744.2	6.62E-17	1.22E-16	protein_coding	417
ASH1L-IT1	ENSG00000227773.1	0	0	sense_intronic	106478976
ASPRV1	ENSG00000244617.2	4.65E-224	4.84E-223	protein_coding	151516
AVPR1B	ENSG00000198049.6	3.47E-167	2.53E-166	protein_coding	553
BDKRB2	ENSG00000168398.6	4.29E-16	7.80E-16	protein_coding	624
BGLT3	ENSG00000260629.1	6.14E-30	1.39E-29	sense_overlapping	103344929
BMP2	ENSG00000125845.6	0.20741731	0.22840266	protein_coding	650
BMP3	ENSG00000152785.6	3.03E-50	8.64E-50	protein_coding	651
BMP5	ENSG00000112175.7	1.08E-39	2.77E-39	protein_coding	653
BMP6	ENSG00000153162.8	1.73E-72	6.08E-72	protein_coding	654
BMP8A	ENSG00000183682.7	3.87E-30	8.78E-30	protein_coding	353500
BPIFB2	ENSG00000078898.6	1.52E-26	3.28E-26	protein_coding	80341
BRAFP1	ENSG00000224775.2	2.35E-44	6.31E-44	unprocessed_pseudogene	286494
C20orf85	ENSG00000124237.5	1.06E-10	1.71E-10	protein_coding	128602
C3AR1	ENSG00000171860.4	1.91E-104	8.87E-104	protein_coding	719
C5	ENSG00000106804.7	3.76E-122	2.00E-121	protein_coding	727
C5AR2	ENSG00000134830.5	4.96E-232	5.45E-231	protein_coding	27202
CALR4P	ENSG00000227742.1	1.05E-174	8.02E-174	unitary_pseudogene	441884
CAMP	ENSG00000164047.4	1.68E-133	9.71E-133	protein_coding	820
CAP1P2	ENSG00000232004.1	1.51E-38	3.79E-38	processed_pseudogene	399748
CAT	ENSG00000121691.4	0.7972736	0.81230185	protein_coding	847
CCL1	ENSG00000108702.3	7.23E-60	2.27E-59	protein_coding	6346
CCL15	ENSG00000275718.1	6.65E-09	1.03E-08	protein_coding	6359
CCL18	ENSG00000275385.1	3.81E-14	6.66E-14	protein_coding	6362
CCL27	ENSG00000213927.3	1.94E-28	4.28E-28	protein_coding	10850
CCL3	ENSG00000277632.1	3.84E-88	1.56E-87	protein_coding	6348
CCL3L3	ENSG00000276085.1	1.30E-37	3.24E-37	protein_coding	414062
CCL4	ENSG00000275302.1	1.66E-134	9.68E-134	protein_coding	6351
CCR1	ENSG00000163823.3	1.72E-88	7.04E-88	protein_coding	1230
CCR10	ENSG00000184451.5	8.46E-21	1.67E-20	protein_coding	2826
CCR4	ENSG00000183813.6	9.66E-76	3.51E-75	protein_coding	1233
CCR7	ENSG00000126353.3	1.14E-121	6.01E-121	protein_coding	1236
CCRL2	ENSG00000121797.9	7.71E-105	3.59E-104	protein_coding	9034
CD180	ENSG00000134061.5	2.00E-27	4.37E-27	protein_coding	4064
CD1A	ENSG00000158477.6	1.63E-21	3.25E-21	protein_coding	909
CD1D	ENSG00000158473.6	1.33E-22	2.71E-22	protein_coding	912
CD81-AS1	ENSG00000238184.1	1.13E-74	4.07E-74	antisense	101927682

CGNL1	ENSG00000128849.10	0.11536106	0.1301156	protein_coding	84952
CHP2	ENSG00000166869.2	1.32E-50	3.78E-50	protein_coding	63928
CLC	ENSG00000105205.6	2.68E-17	4.97E-17	protein_coding	1178
CLDN4	ENSG00000189143.9	2.19E-45	5.94E-45	protein_coding	1364
CLIP1-AS1	ENSG00000257097.1	0	0	lincRNA	100507066
CLP1	ENSG00000172409.5	3.40E-134	1.98E-133	protein_coding	10978
CMTM6	ENSG00000091317.7	5.45E-90	2.25E-89	protein_coding	54918
CNTF	ENSG00000242689.2	9.83E-65	3.23E-64	protein_coding	1270
COLEC12	ENSG00000158270.11	5.64E-06	7.96E-06	protein_coding	81035
CORT	ENSG00000241563.3	3.01E-204	2.78E-203	protein_coding	1325
COTL1	ENSG00000103187.7	7.05E-299	1.19E-297	protein_coding	23406
COX20P1	ENSG00000213025.2	2.82E-38	7.08E-38	processed_pseudogene	100507102
CRABP1	ENSG00000166426.7	2.56E-27	5.58E-27	protein_coding	1381
CRTC3-AS1	ENSG00000259736.1	0	0	antisense	101926895
CSF2	ENSG00000164400.5	8.58E-30	1.94E-29	protein_coding	1437
CSF2RBP1	ENSG00000232254.1	2.55E-18	4.83E-18	unprocessed_pseudogene	23772
CTSLP8	ENSG00000234575.1	7.81E-30	1.76E-29	unprocessed_pseudogene	1518
CX3CL1	ENSG00000006210.6	3.54E-85	1.41E-84	protein_coding	6376
CXCL1	ENSG00000163739.4	2.77E-104	1.28E-103	protein_coding	2919
CXCL2	ENSG00000081041.8	1.23E-05	1.72E-05	protein_coding	2920
CXCL5	ENSG00000163735.6	7.12E-66	2.37E-65	protein_coding	6374
CXCR1	ENSG00000163464.7	0	0	protein_coding	3577
CXCR2P1	ENSG00000229754.1	4.36E-32	1.01E-31	transcribed_unprocessed_pseudogene	3580
CXCR3	ENSG00000186810.7	9.44E-50	2.68E-49	protein_coding	2833
CXCR4	ENSG00000121966.6	1.82E-120	9.52E-120	protein_coding	7852
CXCR5	ENSG00000160683.4	0	0	protein_coding	643
DCDC2B	ENSG00000222046.2	1.52E-128	8.50E-128	protein_coding	149069
DEF6	ENSG00000023892.10	8.28E-300	1.40E-298	protein_coding	50619
DEFA1	ENSG00000206047.2	0	0	protein_coding	1667
DEFA4	ENSG00000164821.4	5.14E-66	1.71E-65	protein_coding	1669
DEFA5	ENSG00000164816.7	1.30E-33	3.08E-33	protein_coding	1670
DEFA6	ENSG00000164822.4	3.00E-13	5.13E-13	protein_coding	1671
DEFB1	ENSG00000164825.3	0.00150982	0.0019319	protein_coding	1672
DEFB108B	ENSG00000184276.2	8.42E-87	3.39E-86	protein_coding	245911
DEFB4A	ENSG00000171711.2	2.94E-08	4.46E-08	protein_coding	1673
DEFB4B	ENSG00000177257.2	0.00014861	0.00019883	protein_coding	100289462
DEFT1P	ENSG00000215378.3	6.98E-89	2.86E-88	unprocessed_pseudogene	170949
DIAPH3-AS2	ENSG00000223815.1	2.97E-115	1.50E-114	antisense	100874196
DIRAS2	ENSG00000165023.5	2.14E-74	7.69E-74	protein_coding	54769
DLL4	ENSG00000128917.6	1.52E-28	3.37E-28	protein_coding	54567
EBI3	ENSG00000105246.5	8.33E-38	2.07E-37	protein_coding	10148
EDN1	ENSG00000078401.6	2.39E-91	9.98E-91	protein_coding	1906
EDNRB-AS1	ENSG00000225579.1	3.20E-22	6.48E-22	lincRNA	100505518
ENDOG	ENSG00000167136.6	1.65E-97	7.23E-97	protein_coding	2021
EREG	ENSG00000124882.3	9.54E-15	1.69E-14	protein_coding	2069
ESRRAP1	ENSG00000215572.2	2.17E-29	4.87E-29	processed_pseudogene	144847
ETAA1	ENSG00000143971.7	1.60E-104	7.40E-104	protein_coding	54465
F2RL1	ENSG00000164251.4	4.15E-20	8.09E-20	protein_coding	2150
FABP2	ENSG00000145384.3	3.94E-14	6.88E-14	protein_coding	2169
FABP7P1	ENSG00000226766.1	8.04E-51	2.31E-50	processed_pseudogene	100506953
FASLG	ENSG00000117560.7	7.85E-91	3.27E-90	protein_coding	356
FGF10	ENSG00000070193.4	2.30E-28	5.09E-28	protein_coding	2255
FGF16	ENSG00000196468.7	1.66E-24	3.46E-24	protein_coding	8823
FGF23	ENSG00000118972.1	6.07E-11	9.87E-11	protein_coding	8074
FGF6	ENSG00000111241.2	2.83E-17	5.25E-17	protein_coding	2251
FGF9	ENSG00000102678.6	2.22E-33	5.23E-33	protein_coding	2254

FGFR3P6	ENSG00000226164.2	5.72E-79	2.15E-78	processed_pseudogene	100420881
FLG	ENSG00000143631.10	4.29E-08	6.48E-08	protein_coding	2312
FLT1P1	ENSG00000229515.1	3.15E-116	1.60E-115	processed_pseudogene	391533
FOSL1P1	ENSG00000248394.1	1.06405054819724e-312	1.93896825096425e-311	processed_pseudogene	100419062
FPR2	ENSG00000171049.8	9.32E-197	8.16E-196	protein_coding	2358
GALR3	ENSG00000128310.2	4.61E-93	1.95E-92	protein_coding	8484
GDF15	ENSG00000130513.6	9.45E-37	2.33E-36	protein_coding	9518
GDF7	ENSG00000143869.6	1.36E-19	2.63E-19	protein_coding	151449
GKN1	ENSG00000169605.5	7.09E-50	2.01E-49	protein_coding	56287
GLP1R	ENSG00000112164.5	1.29E-10	2.07E-10	protein_coding	2740
GMFBP1	ENSG00000243495.1	3.39E-24	7.05E-24	processed_pseudogene	100499251
GNRHR	ENSG00000109163.6	1.09E-281	1.64E-280	protein_coding	2798
GPIHBP1	ENSG00000277494.1	8.34E-30	1.88E-29	protein_coding	338328
GPR135	ENSG00000181619.11	0	0	protein_coding	64582
GPR32	ENSG00000142511.4	1.12E-75	4.08E-75	protein_coding	2854
GPR52	ENSG00000203737.3	8.27E-81	3.16E-80	protein_coding	9293
GREM2	ENSG00000180875.4	1.95E-58	6.05E-58	protein_coding	64388
GRPEL2-AS1	ENSG00000253618.1	2.34E-60	7.39E-60	antisense	106144529
HDAC1P2	ENSG00000233012.2	4.52E-33	1.06E-32	transcribed_processed_pseudogene	100419489
HDGFP1	ENSG00000227183.3	6.76E-122	3.59E-121	processed_pseudogene	474167
HHATL-AS1	ENSG00000230970.3	3.14E-42	8.23E-42	antisense	100874044
HLA-DRB9	ENSG00000196301.3	1.06E-72	3.74E-72	unprocessed_pseudogene	3132
HLA-E	ENSG00000204592.8	0	0	protein_coding	3133
HLA-H	ENSG00000206341.7	2.02E-113	1.00E-112	unprocessed_pseudogene	3136
HRG	ENSG00000113905.4	1.09E-56	3.32E-56	protein_coding	3273
HSPA1A	ENSG00000204389.9	1.27E-286	1.99E-285	protein_coding	3303
HSPA1B	ENSG00000204388.6	2.12E-171	1.59E-170	protein_coding	3304
HSPA1L	ENSG00000204390.9	4.61E-246	5.53E-245	protein_coding	3305
HSPA6	ENSG00000173110.7	0	0	protein_coding	3310
HTR3E-AS1	ENSG00000238020.1	4.20E-39	1.07E-38	antisense	106478970
IFI30	ENSG00000216490.3	0	0	protein_coding	10437
IFITM10	ENSG00000244242.1	3.09E-44	8.28E-44	protein_coding	402778
IFNG	ENSG00000111537.4	2.84E-46	7.79E-46	protein_coding	3458
IFNK	ENSG00000147896.3	2.63E-63	8.53E-63	protein_coding	56832
IFNL2	ENSG00000183709.7	2.99E-32	6.95E-32	protein_coding	282616
IFNL3P1	ENSG00000268510.1	1.16E-17	2.18E-17	unprocessed_pseudogene	100421129
IGHA2	ENSG00000211890.3	9.89E-30	2.23E-29	IG_C_gene	3494
IGHE	ENSG00000211891.5	3.30E-30	7.49E-30	IG_C_gene	3497
IGHJ2	ENSG00000211904.2	5.33E-182	4.27E-181	IG_J_gene	28481
IGHV1-24	ENSG00000211950.2	4.87E-15	8.66E-15	IG_V_gene	28467
IGHV1-3	ENSG00000211935.3	1.81E-32	4.21E-32	IG_V_gene	28473
IGHV1-45	ENSG00000211961.3	9.02E-32	2.09E-31	IG_V_gene	28466
IGHV2-5	ENSG00000211937.3	8.18E-20	1.59E-19	IG_V_gene	28457
IGHV3-35	ENSG00000211957.2	2.46E-76	9.02E-76	IG_V_gene	28432
IGHV3-38	ENSG00000211958.2	5.38E-99	2.39E-98	IG_V_gene	28429
IGHV3-7	ENSG00000211938.2	1.26E-37	3.13E-37	IG_V_gene	28452
IGHV7-81	ENSG00000211979.2	1.02E-115	5.14E-115	IG_V_gene	28378
IGKV1-13	ENSG00000253497.1	5.41E-26	1.16E-25	IG_V_pseudogene	28939
IGKV1-33	ENSG00000242076.2	2.03E-168	1.50E-167	IG_V_gene	28933
IGKV1-37	ENSG00000239862.1	1.56E-35	3.78E-35	IG_V_gene	28931
IGKV1-6	ENSG00000239855.1	6.99E-16	1.27E-15	IG_V_gene	28943
IGKV1-8	ENSG00000240671.2	1.68E-79	6.35E-79	IG_V_gene	28942
IGKV1D-17	ENSG00000242766.1	2.74E-08	4.16E-08	IG_V_gene	28900
IGKV1D-37	ENSG00000250036.1	2.05E-38	5.14E-38	IG_V_gene	28894
IGKV1D-39	ENSG00000251546.1	9.34E-184	7.57E-183	IG_V_gene	28893

IGKV1D-42	ENSG00000211633.3	1.43E-52	4.18E-52	IG_V_gene	28892
IGKV2-24	ENSG00000241294.1	3.61E-18	6.81E-18	IG_V_gene	28923
IGKV2-28	ENSG00000244116.3	9.63E-133	5.53E-132	IG_V_gene	28921
IGKV2-30	ENSG00000243238.1	4.58E-57	1.40E-56	IG_V_gene	28919
IGKV2-40	ENSG00000273962.1	7.17E-25	1.51E-24	IG_V_gene	28916
IGKV2D-28	ENSG00000242534.2	5.05E-24	1.05E-23	IG_V_gene	28883
IGKV2D-29	ENSG00000243264.2	5.14E-17	9.49E-17	IG_V_gene	28882
IGKV2D-30	ENSG00000239571.1	2.09E-19	4.03E-19	IG_V_gene	28881
IGKV3-11	ENSG00000241351.2	2.43E-33	5.73E-33	IG_V_gene	28914
IGKV3-15	ENSG00000244437.1	2.94E-33	6.92E-33	IG_V_gene	28913
IGKV3-7	ENSG00000243063.1	1.05E-49	2.97E-49	IG_V_gene	28915
IGLC2	ENSG00000211677.2	5.28E-36	1.29E-35	IG_C_gene	3538
IGLC3	ENSG00000211679.2	4.86E-36	1.19E-35	IG_C_gene	3539
IGLJ1	ENSG00000211674.2	3.52E-22	7.10E-22	IG_J_gene	28833
IGLJ2	ENSG00000211676.2	6.30E-52	1.83E-51	IG_J_gene	28832
IGLV1-50	ENSG00000211645.2	2.46E-43	6.54E-43	IG_V_gene	28821
IGLV11-55	ENSG00000211641.2	1.20E-19	2.33E-19	IG_V_gene	28770
IGLV2-18	ENSG00000211664.2	3.01E-18	5.70E-18	IG_V_gene	28814
IGLV2-8	ENSG00000278196.1	8.98E-26	1.92E-25	IG_V_gene	28817
IGLV3-32	ENSG00000211657.3	3.43E-18	6.49E-18	IG_V_gene	28787
IKBKGP1	ENSG00000275882.1	5.28E-119	2.73E-118	unprocessed_pseudogene	246210
IL10	ENSG00000136634.5	4.78E-30	1.08E-29	protein_coding	3586
IL17A	ENSG00000112115.5	7.03E-20	1.37E-19	protein_coding	3605
IL17B	ENSG00000127743.5	1.07E-41	2.80E-41	protein_coding	27190
IL1A	ENSG00000115008.5	0.15726375	0.1752618	protein_coding	3552
IL20RB-AS1	ENSG00000249407.1	1.56E-205	1.45E-204	antisense	107986136
IL21R-AS1	ENSG00000259954.1	1.76E-52	5.13E-52	antisense	283888
IL26	ENSG00000111536.4	0.00102991	0.00132776	protein_coding	55801
IL27	ENSG00000197272.2	2.97E-116	1.51E-115	protein_coding	246778
IL31	ENSG00000204671.1	8.59E-60	2.69E-59	protein_coding	386653
IL6STP1	ENSG00000227018.1	5.80E-21	1.15E-20	processed_pseudogene	3573
IL9RP3	ENSG00000226942.2	5.39E-106	2.53E-105	unprocessed_pseudogene	729486
INHBB	ENSG00000163083.5	9.81E-116	4.96E-115	protein_coding	3625
INHBC	ENSG00000175189.3	6.37E-64	2.08E-63	protein_coding	3626
INSL3	ENSG00000248099.3	2.54E-131	1.44E-130	protein_coding	3640
INSL5	ENSG00000172410.4	8.11E-35	1.95E-34	protein_coding	10022
INSL6	ENSG00000120210.6	0	0	protein_coding	11172
JPH2	ENSG00000149596.6	1.18E-98	5.23E-98	protein_coding	57158
JUNB	ENSG00000171223.5	4.04E-122	2.15E-121	protein_coding	3726
KIR3DL3	ENSG00000242019.1	5.95E-21	1.18E-20	protein_coding	115653
KL	ENSG00000133116.7	3.74E-23	7.68E-23	protein_coding	9365
LAP3P1	ENSG00000220091.2	1.66E-51	4.79E-51	processed_pseudogene	100873864
LATS2-AS1	ENSG00000233851.1	0	0	antisense	100874066
LCN1P1	ENSG00000119440.8	1.54E-16	2.81E-16	unprocessed_pseudogene	286310
LCNL1	ENSG00000214402.6	2.16E-07	3.20E-07	protein_coding	401562
LEFTY1	ENSG00000243709.1	1.19E-90	4.95E-90	protein_coding	10637
LEP	ENSG00000174697.4	3.93E-38	9.83E-38	protein_coding	3952
LIF	ENSG00000128342.4	1.20E-40	3.10E-40	protein_coding	3976
LPP-AS1	ENSG00000224563.1	1.57E-55	4.73E-55	antisense	100873917
LTB	ENSG00000227507.2	2.51E-300	4.28E-299	protein_coding	4050
MAP10	ENSG00000212916.4	8.90E-131	5.04E-130	protein_coding	54627
MAP2K1P1	ENSG00000254013.1	3.25E-17	6.02E-17	processed_pseudogene	29778
MAPK8IP2	ENSG00000008735.13	1.35E-34	3.23E-34	protein_coding	23542
MARCO	ENSG00000019169.10	1.92E-62	6.19E-62	protein_coding	8685
MBNL1-AS1	ENSG00000229619.3	5.05E-161	3.54E-160	antisense	401093
MC4R	ENSG00000166603.4	1.92E-13	3.31E-13	protein_coding	4160

MIA-RAB4B	ENSG00000268975.1	4.49E-54	1.33E-53	protein_coding	100529262
MIF	ENSG00000240972.1	3.10E-206	2.89E-205	protein_coding	4282
MLNR	ENSG00000102539.5	1.32E-50	3.77E-50	protein_coding	2862
MMP12	ENSG00000262406.2	1.10E-17	2.05E-17	protein_coding	4321
MMP9	ENSG00000100985.7	9.01E-279	1.33E-277	protein_coding	4318
MPO	ENSG00000005381.7	3.71E-76	1.36E-75	protein_coding	4353
MSH4	ENSG00000057468.6	4.60E-60	1.45E-59	protein_coding	4438
MSTN	ENSG00000138379.4	8.25E-31	1.89E-30	protein_coding	2660
MT2A	ENSG00000125148.6	2.50E-90	1.04E-89	protein_coding	4502
MUC5AC	ENSG00000215182.8	5.44E-29	1.21E-28	protein_coding	4586
MXRA5	ENSG00000101825.7	4.31E-17	7.98E-17	protein_coding	25878
NAMPTP1	ENSG00000229644.6	2.55E-262	3.39E-261	processed_pseudogene	646309
NDP	ENSG00000124479.8	4.85E-20	9.44E-20	protein_coding	4693
NFYAP1	ENSG00000237849.1	3.66E-28	8.08E-28	processed_pseudogene	100130677
NGF	ENSG00000134259.3	2.02E-26	4.34E-26	protein_coding	4803
NNAT	ENSG00000053438.8	6.38E-114	3.18E-113	protein_coding	4826
NOX3	ENSG00000074771.3	3.93E-18	7.41E-18	protein_coding	50508
NPFFR1	ENSG00000148734.7	9.93E-31	2.27E-30	protein_coding	64106
NPR1	ENSG00000169418.9	2.08E-34	4.99E-34	protein_coding	4881
NR0B1	ENSG00000169297.7	1.29E-09	2.02E-09	protein_coding	190
NR0B2	ENSG00000131910.4	2.41E-14	4.22E-14	protein_coding	8431
NRAS	ENSG00000213281.4	6.49E-31	1.49E-30	protein_coding	4893
NSRP1P1	ENSG00000235613.2	0	0	processed_pseudogene	100420557
NTN3	ENSG00000162068.1	3.89E-113	1.93E-112	protein_coding	4917
OPN1SW	ENSG00000128617.2	0	0	protein_coding	611
ORM1	ENSG00000229314.5	5.60E-259	7.29E-258	protein_coding	5004
ORM2	ENSG00000228278.3	1.72E-82	6.67E-82	protein_coding	5005
OSM	ENSG00000099985.3	9.82E-127	5.40E-126	protein_coding	5008
PAK1IP1	ENSG00000111845.4	2.65E-69	9.11E-69	protein_coding	55003
PANK3	ENSG00000120137.6	7.49E-66	2.49E-65	protein_coding	79646
PCSK1N	ENSG00000102109.8	2.37E-103	1.09E-102	protein_coding	27344
PDIA3P2	ENSG00000224677.1	5.36E-105	2.50E-104	unprocessed_pseudogene	106481687
PDSS1P1	ENSG00000182347.10	6.75E-97	2.95E-96	processed_pseudogene	100129248
PF4	ENSG00000163737.3	4.11E-92	1.73E-91	protein_coding	5196
PF4V1	ENSG00000109272.3	1.22E-116	6.23E-116	protein_coding	5197
PGLYRP1	ENSG00000008438.4	3.76E-295	6.19E-294	protein_coding	8993
PHIP	ENSG00000146247.13	5.53E-70	1.91E-69	protein_coding	55023
PI3	ENSG00000124102.4	1.97E-164	1.41E-163	protein_coding	5266
PIK3CD-AS2	ENSG00000231789.2	2.19E-294	3.60E-293	antisense	101929074
PLCG1-AS1	ENSG00000226648.1	3.39E-30	7.69E-30	antisense	101927117
PMP2	ENSG00000147588.6	4.06E-115	2.04E-114	protein_coding	5375
PNPT1P1	ENSG00000229241.1	1.37E-175	1.05E-174	processed_pseudogene	100288506
PNRC1	ENSG00000146278.10	5.32E-222	5.45E-221	protein_coding	10957
PPBP	ENSG00000163736.3	8.44E-55	2.52E-54	protein_coding	5473
PPBPP2	ENSG00000248848.1	6.08E-22	1.22E-21	transcribed_unprocessed_pseudogene	10895
PRF1	ENSG00000180644.6	4.11E-147	2.63E-146	protein_coding	5551
PROK1	ENSG00000143125.5	7.87E-40	2.01E-39	protein_coding	84432
PRSS51	ENSG00000253649.2	4.63E-199	4.13E-198	antisense	346702
PSAPL1	ENSG00000178597.5	6.22E-41	1.61E-40	protein_coding	768239
PSMD6-AS2	ENSG00000239653.1	1.61E-28	3.57E-28	antisense	100507062
PSMD7P1	ENSG00000266707.1	1.19E-31	2.75E-31	processed_pseudogene	280637
PSMD8P1	ENSG00000228264.1	9.59E-29	2.13E-28	processed_pseudogene	100422411
PSME2P2	ENSG00000225131.2	1.13E-231	1.24E-230	processed_pseudogene	338099
PTGDR	ENSG00000168229.3	9.31E-68	3.16E-67	protein_coding	5729
PTGER1	ENSG00000160951.3	1.71E-78	6.41E-78	protein_coding	5731
PTGER4P2	ENSG00000184523.3	3.38E-40	8.67E-40	processed_pseudogene	5736

PTGFRN	ENSG00000134247.9	9.06E-20	1.76E-19	protein_coding	5738
PTX3	ENSG00000163661.3	1.33E-32	3.12E-32	protein_coding	5806
PYY2	ENSG00000237575.4	6.32E-34	1.50E-33	transcribed_unprocessed_pseudogene	23615
QRFP	ENSG00000188710.2	4.41E-73	1.56E-72	protein_coding	347148
RAET1E-AS1	ENSG00000268592.3	1.07E-48	3.01E-48	antisense	100652739
RAI1-AS1	ENSG00000237328.1	0	0	antisense	100861516
RARA-AS1	ENSG00000265666.1	4.7441848314903e-317	8.88325737792099e-316	antisense	101929693
RBP7	ENSG00000162444.11	8.64E-197	7.57E-196	protein_coding	116362
REG1A	ENSG00000115386.5	2.95E-90	1.22E-89	protein_coding	5967
RFPL1S	ENSG00000225465.8	6.14E-31	1.41E-30	antisense	10740
RFXAP	ENSG00000133111.3	1.39E-109	6.72E-109	protein_coding	5994
RHOA-IT1	ENSG00000235908.1	2.54E-49	7.19E-49	sense_intronic	106480739
RORB-AS1	ENSG00000224825.2	2.35E-15	4.21E-15	antisense	103752585
RTP5	ENSG00000188011.5	5.85E-39	1.48E-38	protein_coding	285093
RXRA	ENSG00000186350.9	7.41E-265	1.01E-263	protein_coding	6256
RYKP1	ENSG00000263219.1	0	0	processed_pseudogene	6260
S100A11	ENSG00000163191.5	3.55E-265	4.83E-264	protein_coding	6282
S100A12	ENSG00000163221.8	1.03E-141	6.27E-141	protein_coding	6283
S100A9	ENSG00000163220.10	4.85E-172	3.65E-171	protein_coding	6280
S100G	ENSG00000169906.5	6.67E-291	1.07E-289	protein_coding	795
S100P	ENSG00000163993.6	3.01E-240	3.48E-239	protein_coding	6286
S1PR1	ENSG00000170989.8	2.83E-131	1.61E-130	protein_coding	1901
S1PR2	ENSG00000267534.2	5.78E-41	1.50E-40	protein_coding	9294
SCGB3A1	ENSG00000161055.3	7.85E-35	1.89E-34	protein_coding	92304
SCT	ENSG00000070031.3	2.04E-78	7.62E-78	protein_coding	6343
SEMA3B-AS1	ENSG00000232352.1	3.64E-125	1.98E-124	antisense	101928931
SEMG1	ENSG00000124233.11	3.10E-103	1.42E-102	protein_coding	6406
SERPINA3	ENSG00000273259.2	1.21E-69	4.16E-69	protein_coding	12
SH2D1B	ENSG00000198574.5	1.96E-128	1.09E-127	protein_coding	117157
SHC1P2	ENSG00000267691.1	9.73E-140	5.86E-139	processed_pseudogene	6466
SKA2P1	ENSG00000232387.2	3.98E-59	1.24E-58	processed_pseudogene	729012
SLC10A2	ENSG00000125255.6	6.04E-45	1.63E-44	protein_coding	6555
SLFNL1-AS1	ENSG00000281207.1	9.33E-266	1.27E-264	antisense	100507178
SLPI	ENSG00000124107.5	1.40E-106	6.61E-106	protein_coding	6590
SLURP1	ENSG00000126233.1	8.82E-43	2.33E-42	protein_coding	57152
SOCS1	ENSG00000185338.4	9.81E-117	5.00E-116	protein_coding	8651
SOCS3	ENSG00000184557.4	1.75E-166	1.27E-165	protein_coding	9021
SOD3	ENSG00000109610.5	6.24E-137	3.68E-136	protein_coding	6649
SOS1-IT1	ENSG00000229692.3	5.15E-112	2.54E-111	sense_intronic	100505911
SPR	ENSG00000116096.5	6.53E-46	1.78E-45	protein_coding	6697
SST	ENSG00000157005.3	4.09E-66	1.36E-65	protein_coding	6750
SSTR1	ENSG00000139874.5	6.70E-12	1.11E-11	protein_coding	6751
STK17A	ENSG00000164543.5	0	0	protein_coding	9263
SYNJ2-IT1	ENSG00000233496.1	1.43E-123	7.67E-123	sense_intronic	100874300
TAL2	ENSG00000186051.6	9.44E-24	1.95E-23	protein_coding	6887
TAP1	ENSG00000168394.10	0	0	protein_coding	6890
TECRP2	ENSG00000248565.2	1.27E-39	3.24E-39	processed_pseudogene	391696
TEKT4	ENSG00000163060.7	0.72336772	0.74217599	protein_coding	150483
TGFB2-AS1	ENSG00000232480.1	3.67E-26	7.87E-26	antisense	728463
TGIF2P1	ENSG00000225401.2	0	0	transcribed_processed_pseudogene	126826
THBS1	ENSG00000137801.10	4.96E-32	1.15E-31	protein_coding	7057
THRAP3P1	ENSG00000227339.1	2.36E-89	9.70E-89	processed_pseudogene	391524
THRB-IT1	ENSG00000224822.1	2.13E-25	4.52E-25	sense_intronic	100874274
TLL2	ENSG00000095587.8	9.81E-43	2.59E-42	protein_coding	7093
TLR2	ENSG00000137462.6	6.54E-196	5.69E-195	protein_coding	7097

TLR4	ENSG00000136869.13	2.16E-71	7.53E-71	protein_coding	7099
TLR8	ENSG00000101916.11	4.67E-64	1.52E-63	protein_coding	51311
TMSB10P1	ENSG00000228499.1	4.13E-229	4.45E-228	processed_pseudogene	100506723
TMSB4XP8	ENSG00000187653.11	3.29E-279	4.87E-278	processed_pseudogene	7117
TNF	ENSG00000232810.3	3.73E-32	8.67E-32	protein_coding	7124
TNFRSF13C	ENSG00000159958.4	4.93E-115	2.48E-114	protein_coding	115650
TNFRSF21	ENSG00000146072.6	1.27E-16	2.32E-16	protein_coding	27242
TNFSF12-TNFSF13	ENSG00000248871.1	2.49E-279	3.69E-278	protein_coding	407977
TRAJ10	ENSG00000211879.1	2.14E-76	7.84E-76	TR_J_gene	28745
TRAV1-1	ENSG00000255569.1	8.06E-43	2.13E-42	TR_V_gene	28693
TRAV1-2	ENSG00000256553.1	6.96E-44	1.86E-43	TR_V_gene	28692
TRAV10	ENSG00000211784.2	2.22E-56	6.75E-56	TR_V_gene	28676
TRAV12-1	ENSG00000211785.1	3.41E-47	9.42E-47	TR_V_gene	28674
TRAV12-2	ENSG00000211789.2	2.15E-69	7.38E-69	TR_V_gene	28673
TRAV12-3	ENSG00000211794.3	3.74E-67	1.26E-66	TR_V_gene	28672
TRAV13-1	ENSG00000211788.2	3.71E-54	1.10E-53	TR_V_gene	28671
TRAV13-2	ENSG00000211791.2	2.40E-65	7.93E-65	TR_V_gene	28670
TRAV14DV4	ENSG00000211792.2	2.40E-53	7.09E-53	TR_V_gene	28669
TRAV16	ENSG00000211796.1	1.29E-30	2.94E-30	TR_V_gene	28667
TRAV17	ENSG00000211797.2	1.42E-58	4.40E-58	TR_V_gene	28666
TRAV18	ENSG00000211798.3	1.24E-43	3.29E-43	TR_V_gene	28665
TRAV19	ENSG00000211799.3	2.46E-62	7.93E-62	TR_V_gene	28664
TRAV2	ENSG00000211776.2	1.88E-66	6.29E-66	TR_V_gene	28691
TRAV20	ENSG00000211800.3	1.49E-55	4.49E-55	TR_V_gene	28663
TRAV21	ENSG00000211801.3	4.50E-42	1.18E-41	TR_V_gene	28662
TRAV23DV6	ENSG00000211803.2	8.06E-53	2.36E-52	TR_V_gene	28660
TRAV24	ENSG00000211805.1	7.81E-33	1.83E-32	TR_V_gene	28659
TRAV25	ENSG00000211806.2	5.17E-50	1.47E-49	TR_V_gene	28658
TRAV26-1	ENSG00000211807.3	1.67E-56	5.08E-56	TR_V_gene	28657
TRAV27	ENSG00000211809.2	1.03E-26	2.23E-26	TR_V_gene	28655
TRAV29DV5	ENSG00000211810.3	7.60E-45	2.05E-44	TR_V_gene	28653
TRAV3	ENSG00000211777.2	1.12E-56	3.40E-56	TR_V_gene	28690
TRAV4	ENSG00000211778.2	7.60E-66	2.52E-65	TR_V_gene	28689
TRAV5	ENSG00000211779.3	2.47E-33	5.84E-33	TR_V_gene	28688
TRAV6	ENSG00000211780.3	1.20E-27	2.63E-27	TR_V_gene	6956
TRAV8-1	ENSG00000211782.2	8.43E-71	2.93E-70	TR_V_gene	28685
TRAV8-2	ENSG00000211786.3	1.81E-77	6.69E-77	TR_V_gene	28684
TRAV8-4	ENSG00000211790.2	3.10E-60	9.78E-60	TR_V_gene	28682
TRAV8-6	ENSG00000211795.3	4.36E-62	1.40E-61	TR_V_gene	28680
TRAV9-2	ENSG00000211793.2	2.48E-65	8.21E-65	TR_V_gene	28677
TRBV10-2	ENSG00000229769.2	1.40E-18	2.66E-18	TR_V_gene	28584
TRBV10-3	ENSG00000275791.1	1.10E-40	2.85E-40	TR_V_gene	28583
TRBV11-2	ENSG00000241657.1	3.14E-63	1.02E-62	lincRNA	28581
TRBV12-4	ENSG00000276953.1	4.69E-55	1.41E-54	TR_V_gene	28576
TRBV14	ENSG00000275743.1	2.11E-48	5.90E-48	TR_V_gene	28573
TRBV15	ENSG00000276819.1	8.65E-57	2.64E-56	TR_V_gene	28572
TRBV17	ENSG00000277880.1	6.00E-41	1.55E-40	TR_V_gene	28570
TRBV18	ENSG00000276557.1	7.50E-79	2.82E-78	TR_V_gene	28569
TRBV19	ENSG00000211746.3	1.74E-93	7.40E-93	TR_V_gene	28568
TRBV2	ENSG00000226660.2	3.42E-68	1.16E-67	TR_V_gene	28620
TRBV20-1	ENSG00000211747.3	1.04E-42	2.75E-42	TR_V_gene	28567
TRBV24-1	ENSG00000211750.2	3.15E-56	9.54E-56	TR_V_gene	28563
TRBV29-1	ENSG00000232869.2	4.84E-117	2.47E-116	TR_V_gene	28558
TRBV3-1	ENSG00000237702.2	1.30E-76	4.76E-76	TR_V_gene	28619
TRBV30	ENSG00000237254.2	1.06E-57	3.26E-57	TR_V_gene	28557

TRBV4-1	ENSG00000211710.3	6.83E-58	2.10E-57	TR_V_gene	28617
TRBV4-2	ENSG00000211745.3	3.76E-61	1.20E-60	TR_V_gene	28616
TRBV5-1	ENSG00000211734.3	2.75E-104	1.27E-103	TR_V_gene	28614
TRBV5-6	ENSG00000211728.2	1.07E-23	2.20E-23	TR_V_gene	28609
TRBV5-7	ENSG00000211731.1	1.47E-124	7.96E-124	TR_V_gene	28608
TRBV6-1	ENSG00000211706.2	6.11E-77	2.25E-76	TR_V_gene	28606
TRBV6-5	ENSG00000211721.2	3.06E-05	4.20E-05	TR_V_gene	28602
TRBV6-7	ENSG00000253188.1	1.05E-96	4.60E-96	TR_V_gene	28600
TRBV6-8	ENSG00000253534.1	1.44E-90	5.99E-90	TR_V_gene	28599
TRBV7-3	ENSG00000211714.3	4.68E-37	1.16E-36	TR_V_gene	28595
TRBV7-4	ENSG00000253409.1	8.05E-45	2.17E-44	TR_V_gene	28594
TRBV7-7	ENSG00000253291.1	3.22E-24	6.71E-24	TR_V_gene	28591
TRBV7-9	ENSG00000278030.1	7.98E-55	2.39E-54	TR_V_gene	28589
TRBV9	ENSG00000211716.2	1.60E-57	4.93E-57	TR_V_gene	28586
TRDV1	ENSG00000211804.3	5.05E-46	1.38E-45	TR_V_gene	28518
TRDV3	ENSG00000256590.2	2.17E-16	3.96E-16	TR_V_gene	28516
TRGJP2	ENSG00000211688.1	1.09E-297	1.83E-296	TR_J_gene	6972
TRGV5P	ENSG00000228668.1	6.84E-21	1.35E-20	TR_V_pseudogene	6979
TRH	ENSG00000170893.3	1.89E-111	9.27E-111	protein_coding	7200
TRHR	ENSG00000174417.2	2.33E-89	9.57E-89	protein_coding	7201
TRIM58	ENSG00000162722.8	1.08E-44	2.91E-44	protein_coding	25893
TUBB3	ENSG00000198211.8	1.17E-78	4.39E-78	protein_coding	10381
ULBP2	ENSG00000131015.4	1.10E-19	2.13E-19	protein_coding	80328
UNC93B4	ENSG00000250381.1	2.36E-22	4.79E-22	unprocessed_pseudogene	643384
UTS2R	ENSG00000181408.3	3.64E-21	7.21E-21	protein_coding	2837
VAV3-AS1	ENSG00000230489.1	4.19E-59	1.31E-58	antisense	100873946
VEGFC	ENSG00000150630.3	0.09146515	0.10412237	protein_coding	7424
VIM2P	ENSG00000220548.3	3.09E-44	8.28E-44	processed_pseudogene	100130535
WFIKKN2	ENSG00000173714.7	5.62E-58	1.73E-57	protein_coding	124857
XCL1	ENSG00000143184.4	6.83E-80	2.59E-79	protein_coding	6375
XCL2	ENSG00000143185.3	6.67E-87	2.69E-86	protein_coding	6846
XCR1	ENSG00000173578.7	1.28E-48	3.60E-48	protein_coding	2829
ZC3HAV1L	ENSG00000146858.7	0	0	protein_coding	92092

Table S2. Results of GSEA pathway enrichment with immunologic signature gene sets

Description	setSize	enrichmentScore	NES	*p* value	p.adjust	q values	rank	leading_edge	core_enrichment
GSE34205_HEALTHY_VS_RSV_INF_INFANT_PBMC_DN	12	-0.86396	-2.63336	3.24E-08	3.02E-06	1.40E-06	42	tags=83%, list=10%, signal=77%	SLPI/DEFA4/S100A9/S100A12/S100P/TUBB3/CAMP/PGLYRP1/ORM1/MMP9
GSE4748_CYANOBACTERIUM_LPSLIKE_VS_LPS_AND_CYANOBACTERIUM_LPSLIKE_STIM_DC_3H_DN	11	-0.84871	-2.52432	1.57E-07	7.30E-06	3.39E-06	42	tags=82%, list=10%, signal=76%	SLPI/DEFA4/INHBB/S100A11/S100A9/TUBB3/CAMP/PGLYRP1/MMP9
GSE22886_NAIVE_BCELL_VS_NEUTROPHIL_DN	11	-0.84219	-2.50492	2.96E-07	9.16E-06	4.25E-06	65	tags=91%, list=15%, signal=79%	CXCL1/SLPI/S100A11/S100A9/S100A12/S100P/CAMP/HSPA1A/HSPA6/CXCR1
GSE6269_E_COLI_VS_STREP_PNEUMO_INF_PBMC_DN	10	-0.83563	-2.40772	2.36E-06	5.49E-05	2.55E-05	42	tags=70%, list=10%, signal=65%	SLPI/S100A9/S100P/CAMP/PGLYRP1/ORM1/MMP9
GSE360_CTRL_VS_M_TUBERCULOSIS_DC_DN	14	-0.74281	-2.37666	7.59E-06	0.000141	6.55E-05	106	tags=93%, list=25%, signal=72%	C3AR1/MMP12/CCR7/MT2A/MARCO/IFNG/SLPI/S100A11/CCL3/CCL4/S100A9/TUBB3/MMP9
GSE360_LOW_DOSE_B_MALAYI_VS_M_TUBERCULOSIS_DC_DN	13	-0.73246	-2.28377	5.60E-05	0.000803	0.000372	106	tags=92%, list=25%, signal=71%	C3AR1/MMP12/CCR7/CSF2/MT2A/CXCL5/MARCO/CCL3/S100A9/TUBB3/HSPA1A/MMP9
GSE45365_NK_CELL_VS_CD11B_DC_DN	13	-0.73132	-2.28021	6.04E-05	0.000803	0.000372	65	tags=69%, list=15%, signal=60%	CXCL1/OSM/LIF/INHBB/FPR2/CCL4/S100A9/PGLYRP1/MMP9
GSE360_HIGH_DOSE_B_MALAYI_VS_M_TUBERCULOSIS_DC_DN	12	-0.75573	-2.30349	7.89E-05	0.000918	0.000426	95	tags=92%, list=23%, signal=73%	MMP12/CCR7/MT2A/CXCL5/SOD3/IFNG/S100A11/CCL4/S100A9/TUBB3/MMP9
NAKAYA_PBMC_FLUMIST_AGE_18_50YO_7DY_DN	20	-0.62504	-2.2133	0.000208	0.002035	0.000944	101	tags=60%, list=24%, signal=48%	PPBP/CXCR4/SOCS3/CXCL1/OSM/PF4/FPR2/S100P/CXCR5/MMP9/CXCR1/DEFA1
ZAK_PBMC_MRKAD5_HIV_1_GAG_POL_NEF_AGE_20_50YO_1DY_UP	21	-0.60186	-2.17798	0.000219	0.002035	0.000944	148	tags=86%, list=35%, signal=58%	TLR4/SOCS1/CCR1/IL27/C3AR1/TAP1/MT2A/RXRA/TLR8/SOCS3/MARCO/TLR2/S100A11/FPR2/CCL3/S100A9/IFI30/HSPA6
GSE3039_ALPHAALPHA_VS_ALPHABETA_CD8_TCELL_UP	10	-0.74785	-2.15479	0.000263	0.002227	0.001033	89	tags=90%, list=21%, signal=73%	MT2A/SOCS3/TLR2/CXCL1/OSM/PF4/CCL4/HSPA1B/HSPA1A
HOWARD_PBMC_INACT_MONOV_INFLUENZA_A_INDONESIA_05_2005_H5N1_AGE_19_39YO_AS03_ADJUVANT_VS_BUFFER_1DY_UP	18	-0.63946	-2.1966	0.000342	0.002653	0.001231	126	tags=83%, list=30%, signal=61%	CCR1/IL27/C3AR1/PSME2P2/TAP1/MT2A/SOCS3/MARCO/TLR2/FPR2/S100A9/S100A12/NAMPTP1/IFI30/HSPA6
GSE22886_NAIVE_CD4_TCELL_VS_NEUTROPHIL_DN	11	-0.72245	-2.14879	0.000418	0.002774	0.001287	85	tags=73%, list=20%, signal=60%	CHP2/CXCL1/C5AR2/S100A9/S100A12/S100P/HSPA1A/HSPA6
GSE22886_NAIVE_CD8_TCELL_VS_NEUTROPHIL_DN	11	-0.72222	-2.14811	0.000418	0.002774	0.001287	85	tags=82%, list=20%, signal=67%	CHP2/CXCL1/LIF/C5AR2/S100A9/S100A12/S100P/CAMP/HSPA6
GSE36888_UNTREATED_VS_IL2_TREATED_STAT5_AB_KNOCKIN_TCELL_2H_UP	13	-0.67947	-2.11853	0.000562	0.003485	0.001617	76	tags=62%, list=18%, signal=52%	SOCS3/CXCL5/TLR2/CXCL1/FPR2/CCL4/S100A9/S100A12
GSE22886_NEUTROPHIL_VS_DC_UP	11	-0.71161	-2.11654	0.000617	0.00354	0.001643	65	tags=73%, list=15%, signal=63%	CXCL1/LTB/C5AR2/PRF1/S100A12/S100P/CAMP/CXCR1

HARALAMBIEVA_PBMC_M_M_R_II_AGE_11_22YO_VACCINATED_VS_UNVACCINATED_7YR_DN	19	-0.61974	-2.15821	0.000647	0.00354	0.001643	105	tags=58%, list=25%, signal=45%	S1PR1/PPBP/RXRA/CXCL5/COTL1/LEP/CXCL1/S100A9/S100A12/TNFSF12-TNFSF13/MMP9
SCHERER_PBMC_APSV_WETVAX_AGE_18_32YO_5_TO_7DY_UP	10	-0.71951	-2.07314	0.000778	0.003921	0.00182	126	tags=100%, list=30%, signal=72%	C3AR1/TAP1/TLR8/SOCS3/MARCO/TLR2/FPR2/S100A9/IFI30
ZAK_PBMC_MRKAD5_HIV_1_GAG_POL_NEF_AGE_20_50YO_1DY_DN	51	-0.45877	-2.04615	0.000801	0.003921	0.00182	207	tags=90%, list=49%, signal=52%	TRAV29DV5/TRBV20-1/TRAV21/TRAV24/PNRC1/TRAV16/TRAV5/TRAV1-2/STK17A/TRAV12-1/TRAV25/TRAV13-1/TRAV26-1/CCR4/TRBV11-2/TRBV9/TRAV9-2/TRAV20/TRAV14DV4/TRAV17/TRAV23DV6/PTGDR/TRAV13-2/TRAV3/TRAV8-6/TRBV2/TRAV4/TRBV24-1/TRAV12-2/TRAV19/TRBV4-2/TRAV12-3/TRBV6-1/TRAV2/TRDV1/S1PR1/TRBV3-1/TRAV8-1/CXCR4/TRBV19/CCR7/TRBV5-1/TRAV8-2/SH2D1B/LTB/CXCR5
OSMAN_BLOOD_CHAD63_KH_AGE_18_50YO_HIGH_DOSE_SUBJECTS_24HR_UP	37	-0.48064	-1.98226	0.000985	0.00458	0.002126	126	tags=57%, list=30%, signal=44%	CCR1/IL27/HLA-H/C3AR1/TAP1/MT2A/TLR8/MARCO/TLR2/COTL1/HLA-E/OSM/LIF/ARAP1-AS1/ASPRV1/FPR2/HSPA1B/HSPA1A/IFI30/HSPA6/CXCR1
GSE22886_NAIVE_TCELL_VS_NEUTROPHIL_DN	11	-0.69172	-2.05738	0.001241	0.005496	0.002551	85	tags=73%, list=20%, signal=60%	CHP2/TLR8/CXCL1/C5AR2/SLPI/S100A12/S100P/CXCR1
FOURATI_BLOOD_TWINRIX_AGE_25_83YO_RESPONDERS_VS_POOR_RESPONDERS_0DY_DN	14	-0.63985	-2.04721	0.001362	0.005756	0.002671	42	tags=43%, list=10%, signal=40%	SLPI/DEFA4/RBP7/CAMP/HSPA1B/DEFA1
GSE9006_HEALTHY_VS_TYPE_1_DIABETES_PBMC_AT_DX_DN	15	-0.62273	-2.02254	0.001894	0.007658	0.003554	106	tags=73%, list=25%, signal=57%	CCR1/C3AR1/S1PR1/CCR7/SOCS3/CXCL1/SLPI/FPR2/S100P/PI3/CXCR1
GSE19401_NAIVE_VS_IMMUNIZED_MOUSE_PLN_FOLLICULAR_DC_UP	11	-0.66733	-1.98486	0.002898	0.01123	0.005211	65	tags=55%, list=15%, signal=47%	CXCL1/CCL3/CCL4/S100A9/S100A12/HSPA1A
HOEK_NK_CELL_2011_2012_TIV_3D_VS_0DY_ADULT_3D_DN	12	-0.65294	-1.99018	0.003111	0.011571	0.00537	81	tags=67%, list=19%, signal=55%	TLR8/TLR2/OSM/RBP7/S100A9/S100A12/TNFSF12-TNFSF13/IFI30
GSE36888_UNTREATED_VS_IL2_TREATED_TCELL_17H_DN	12	-0.64483	-1.96546	0.004215	0.015077	0.006997	89	tags=67%, list=21%, signal=54%	MT2A/CXCL5/TLR2/CXCL1/FPR2/CCL4/S100A12/TUBB3
GSE25123_WT_VS_PPARG_KO_MACROPHAGE_UP	10	-0.6719	-1.93596	0.004702	0.016194	0.007515	76	tags=60%, list=18%, signal=50%	SOCS3/OSM/FPR2/HSPA1A/ORM1/HSPA6
HARALAMBIEVA_PBMC_FLUARIX_AGE_50_74YO_CORR_WITH_28D_MEM_B_CELL_RESPONSE_AT_28DY_POSITIVE	21	-0.51734	-1.87212	0.005619	0.018663	0.008661	71	tags=38%, list=17%, signal=33%	COTL1/OSM/C5AR2/FPR2/TUBB3/TNFSF12-TNFSF13/IFI30/MMP9
GSE22886_DAY0_VS_DAY1_MONOCYTE_IN_CULTURE_DN	10	-0.64725	-1.86494	0.00887	0.028444	0.0132	101	tags=70%, list=24%, signal=54%	PPBP/CCR7/MT2A/CXCL1/CCL4/MMP9/PI3

GARCIA_PINERES_PBMC_HPV_16_L1_VLP_AGE_18_25YO_STIMULATED_VS_UNSTIMULATED_0DY_VACCINATION_INDEPENDENT_UP	12	-0.61447	-1.87293	0.00964	0.029885	0.013869	90	tags=67%, list=21%, signal=54%	SLURP1/MT2A/CXCL1/LIF/IFNG/FPR2/CCL3/MMP9
GSE41087_WT_VS_FOXP3_MUT_ANTI_CD3_CD28_STIM_CD4_TCELL_UP	11	-0.62865	-1.86979	0.010426	0.031277	0.014515	100	tags=73%, list=24%, signal=57%	CXCR4/CCR7/TLR8/HLA-E/PF4/C5AR2/S100A12/S100P
GSE7218_UNSTIM_VS_ANTIGEN_STIM_THROUGH_IGG_BCELL_DN	10	-0.63523	-1.8303	0.011768	0.032442	0.015055	92	tags=70%, list=22%, signal=56%	CCR7/CSF2/SLPI/PRF1/CCL3/S100A9/PGLYRP1
NAKAYA_MONOCYTE_FLUMIST_AGE_18_50YO_7DY_UP	10	-0.63608	-1.83274	0.011768	0.032442	0.015055	81	tags=60%, list=19%, signal=50%	TLR8/CXCL1/CCL3/CCL4/HSPA1B/HSPA1A
GSE14769_UNSTIM_VS_80MIN_LPS_BMDM_DN	13	-0.57986	-1.80796	0.011861	0.032442	0.015055	73	tags=46%, list=17%, signal=39%	TLR2/CXCL1/OSM/CCL4/HSPA1B/HSPA1A
GSE14769_UNSTIM_VS_60MIN_LPS_BMDM_DN	11	-0.62093	-1.84684	0.012526	0.033283	0.015445	73	tags=55%, list=17%, signal=46%	TLR2/CXCL1/OSM/CCL4/HSPA1B/HSPA1A
GARCIA_PINERES_PBMC_HPV_16_L1_VLP_AGE_18_25YO_2MO_UP	16	-0.54461	-1.79967	0.013085	0.033803	0.015687	95	tags=62%, list=23%, signal=50%	MMP12/CSF2/MT2A/TLR2/FASLG/LIF/XCL1/IFNG/FPR2/CCL4

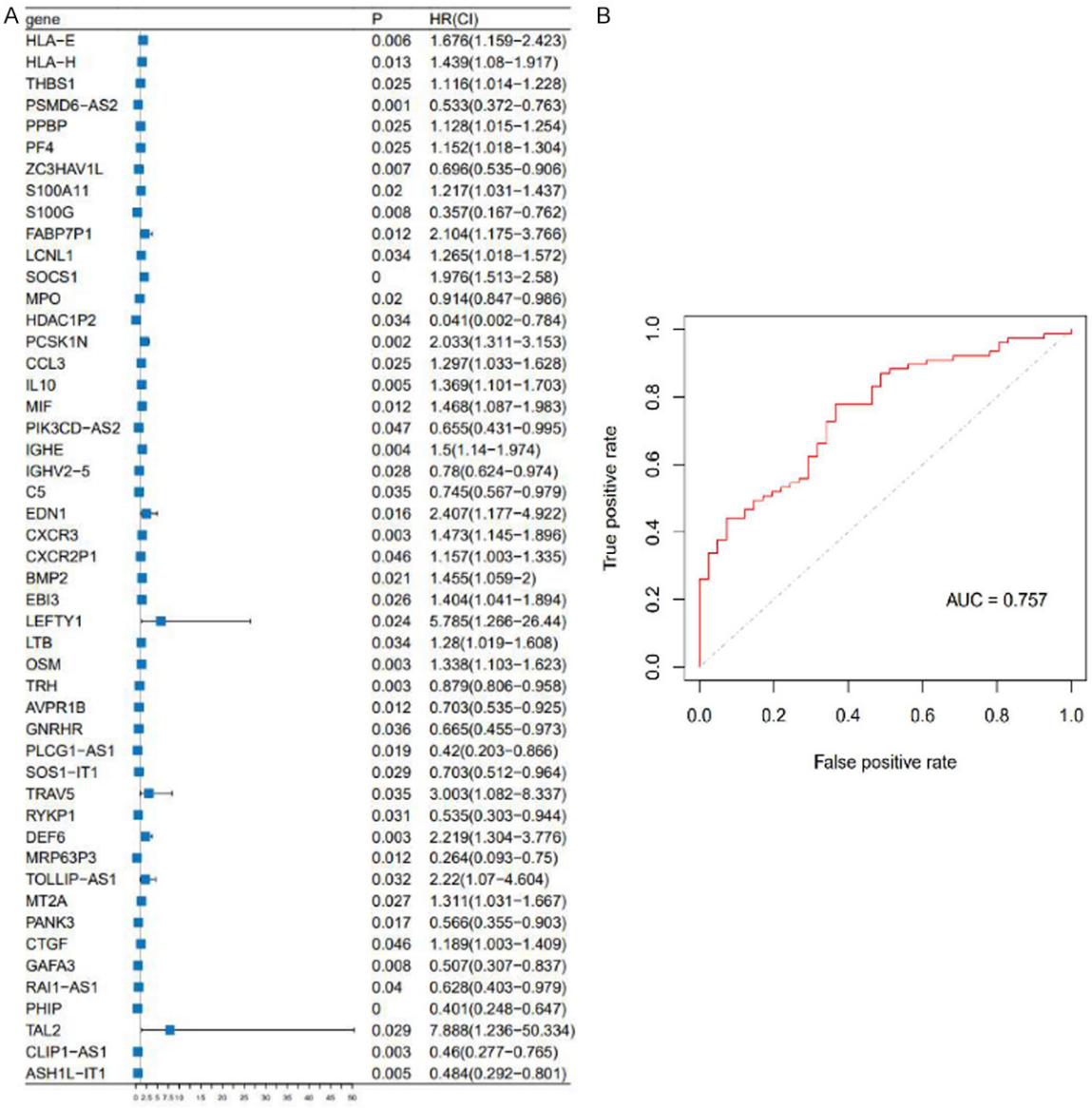

Figure S1. Construction of an immune-related AML prognostic model. A. Univariate Cox regression analysis of AML-immune-related DEGs (*P* value < 0.05); B. ROC of Lasso regression.

Table S3. Supplemental data for univariate Cox regression analysis

	coef	se	z	p	HR	HRse	HRz	HRp	HRCILL	HRCIUL
HLA-E	0.516	0.188	2.745	0.006	1.676	0.315	2.144	0.032	1.159	2.423
HLA-H	0.364	0.146	2.487	0.013	1.439	0.21	2.085	0.037	1.08	1.917
THBS1	0.11	0.049	2.237	0.025	1.116	0.055	2.119	0.034	1.014	1.228
PSMD6-AS2	-0.629	0.183	-3.435	0.001	0.533	0.098	-4.783	0	0.372	0.763
PPBP	0.121	0.054	2.239	0.025	1.128	0.061	2.109	0.035	1.015	1.254
PF4	0.142	0.063	2.248	0.025	1.152	0.073	2.096	0.036	1.018	1.304
ZC3HAV1L	-0.362	0.135	-2.693	0.007	0.696	0.094	-3.245	0.001	0.535	0.906
S100A11	0.197	0.085	2.325	0.02	1.217	0.103	2.111	0.035	1.031	1.437
S100G	-1.03	0.387	-2.662	0.008	0.357	0.138	-4.654	0	0.167	0.762
FABP7P1	0.744	0.297	2.504	0.012	2.104	0.625	1.766	0.077	1.175	3.766

LCNL1	0.235	0.111	2.124	0.034	1.265	0.14	1.892	0.058	1.018	1.572
SOCS1	0.681	0.136	4.999	0	1.976	0.269	3.626	0	1.513	2.58
MPO	-0.09	0.039	-2.318	0.02	0.914	0.035	-2.425	0.015	0.847	0.986
HDAC1P2	-3.189	1.503	-2.122	0.034	0.041	0.062	-15.475	0	0.002	0.784
PCSK1N	0.71	0.224	3.171	0.002	2.033	0.455	2.271	0.023	1.311	3.153
CCL3	0.26	0.116	2.236	0.025	1.297	0.151	1.969	0.049	1.033	1.628
IL10	0.314	0.111	2.822	0.005	1.369	0.152	2.421	0.015	1.101	1.703
MIF	0.384	0.153	2.504	0.012	1.468	0.225	2.079	0.038	1.087	1.983
PIK3CD-AS2	-0.423	0.214	-1.983	0.047	0.655	0.14	-2.469	0.014	0.431	0.995
IGHE	0.406	0.14	2.894	0.004	1.5	0.21	2.379	0.017	1.14	1.974
IGHV2-5	-0.249	0.113	-2.194	0.028	0.78	0.088	-2.491	0.013	0.624	0.974
C5	-0.295	0.139	-2.114	0.035	0.745	0.104	-2.458	0.014	0.567	0.979
EDN1	0.878	0.365	2.407	0.016	2.407	0.879	1.602	0.109	1.177	4.922
CXCR3	0.388	0.129	3.011	0.003	1.473	0.19	2.496	0.013	1.145	1.896
CXCR2P1	0.146	0.073	1.995	0.046	1.157	0.085	1.857	0.063	1.003	1.335
BMP2	0.375	0.162	2.312	0.021	1.455	0.236	1.928	0.054	1.059	2
EBI3	0.339	0.153	2.22	0.026	1.404	0.214	1.883	0.06	1.041	1.894
LEFTY1	1.755	0.775	2.264	0.024	5.785	4.485	1.067	0.286	1.266	26.44
LTB	0.247	0.117	2.117	0.034	1.28	0.149	1.876	0.061	1.019	1.608
OSM	0.291	0.099	2.95	0.003	1.338	0.132	2.56	0.01	1.103	1.623
TRH	-0.129	0.044	-2.929	0.003	0.879	0.039	-3.127	0.002	0.806	0.958
AVPR1B	-0.352	0.14	-2.518	0.012	0.703	0.098	-3.018	0.003	0.535	0.925
GNRHR	-0.408	0.194	-2.102	0.036	0.665	0.129	-2.596	0.009	0.455	0.973
PLCG1-AS1	-0.868	0.37	-2.349	0.019	0.42	0.155	-3.74	0	0.203	0.866
SOS1-IT1	-0.353	0.161	-2.188	0.029	0.703	0.113	-2.624	0.009	0.512	0.964
TRAV5	1.1	0.521	2.111	0.035	3.003	1.565	1.28	0.2	1.082	8.337
RYKP1	-0.626	0.29	-2.158	0.031	0.535	0.155	-2.999	0.003	0.303	0.944
DEF6	0.797	0.271	2.938	0.003	2.219	0.602	2.025	0.043	1.304	3.776
MRP63P3	-1.333	0.533	-2.5	0.012	0.264	0.141	-5.236	0	0.093	0.75
TOLLIP-AS1	0.797	0.372	2.143	0.032	2.22	0.826	1.477	0.14	1.07	4.604
MT2A	0.271	0.123	2.205	0.027	1.311	0.161	1.932	0.053	1.031	1.667
PANK3	-0.569	0.239	-2.386	0.017	0.566	0.135	-3.214	0.001	0.355	0.903
CTGF	0.173	0.087	1.991	0.046	1.189	0.103	1.828	0.067	1.003	1.409
GAFA3	-0.679	0.256	-2.653	0.008	0.507	0.13	-3.799	0	0.307	0.837
RAI1-AS1	-0.466	0.227	-2.054	0.04	0.628	0.142	-2.616	0.009	0.403	0.979
PHIP	-0.915	0.244	-3.745	0	0.401	0.098	-6.125	0	0.248	0.647
TAL2	2.065	0.946	2.184	0.029	7.888	7.459	0.923	0.356	1.236	50.334
CLIP1-AS1	-0.776	0.259	-2.997	0.003	0.46	0.119	-4.529	0	0.277	0.765
ASH1L-IT1	-0.726	0.257	-2.825	0.005	0.484	0.124	-4.152	0	0.292	0.801